Bulletin of the Seismological Society of America. Vol. 59, No. 1, pp. 101–130. February, 1969

CRUSTAL STRUCTURE OF THE ISLAND OF HAWAII FROM SEISMIC-REFRACTION MEASUREMENTS*

By David P. Hill†

ABSTRACT

In August of 1964 the U. S. Geological Survey established seismic-refraction profiles along the northeast, southwest, and west coasts of the roughly triangular-shaped Island of Hawaii. Shots were fired at 10-km intervals along each coast from the U. S. Coast Guard Cutter CAPE SMALL and were recorded on shore by five refraction units spaced at approximately 25 km intervals along each coast. Most of these shots were also recorded on the 13 seismograph stations maintained on Hawaii by the U. S. Geological Survey's Hawaiian Volcano Observatory. These data were supplemented by recordings on the 13-station seismograph network and two mobile systems of three 500-ton chemical explosions detonated by the U. S. Navy on Kahoolawe as part of the SAILOR HAT program and by a re-evaluation of arrivals recorded on the seismograph network from seismic-refraction profiles shot off the northeast coast of Hawaii by Scripps Institution of Oceanography in 1962.

Interpretation of the resulting seismograms suggests that the crust under Hawaii can be divided into two principal layers: (1) a basal layer 4 to 8 km thick with *P*-wave velocities of 7.0 to 7.2 km/sec, and (2) an upper layer 4 to 8 km thick in which *P*-wave velocities increase with depth from 1.8 to 3.3 km/sec at the surface to 5.1 to 6.0 km/sec at depth. The basal layer is probably the original oceanic crust under Hawaii plus the intrusive system associated with central vents and rift zones, and the upper layer is the accumulated pile of lava flows that form the bulk of the island.

The crust along the northeast and southwest flanks of Kilauea is 11 to 12 km thick with *P*-wave velocities increasing in the upper layer from 1.8 km/sec at the surface to 5.1 km/sec at depth. The basal layer is 4 km thick and has a *P*-wave velocity of 7.1 km/sec. A 7.0-km/sec layer at depths of 3 to 5 km under the northeast flanks of Mauna Kea and Kohala Mountain masks first-arrival evidence for deeper structure, but secondary arrivals interpreted as reflections from the M discontinuity suggest that the underlying crust may be anywhere between 12 and 20 km thick. This shallow 7.0-km/sec layer is probably associated with the nearby rift zones of Kohala Mountain and Mauna Kea. The crust increases in thickness along the west coast of Hawaii from about 14 km under the flanks of Kohala Mountain and Hualalai to about 18 km under the flank of Mauna Loa. *P*-wave velocities along this coast increase with depth from 2.5 km/sec at the surface to 6.0 km/sec at about 10 km, and the lower 4 to 6 km of the crust has a *P*-wave velocity of about 7.2 km/sec. The upper mantle *P*-wave velocity under most of the island is 8.2 km/sec but may decrease to 8.1 km/sec under the southeast flank of Kilauea. Material with mantle-like *P*-wave velocity appears to bulge up under the summit of Kilauea to a depth as shallow as 10 or 11 km.

Early *P*-wave arrivals associated with the summits and major rift zones of the volcanoes indicate that material with velocities as high as 7.0 km/sec approaches within 2 or 3 km of the surface under these structures and merges at depth with the 7.1- to 7.2-km/sec layer forming the base of the crust.

* Publication authorized by the Director, U. S. Geological Survey.
† Presently at California Institute of Technology, Pasadena, Calif.

Introduction

In recent years the U. S. Geological Survey at the Hawaiian Volcano Observatory (HVO) has given increasing emphasis to the study of local earthquakes and their relation to crustal structure and geologic processes of the active volcanoes of Hawaii. In an effort to further define the crustal structure and travel-time curves, the U. S. Geological Survey, with the support of the U. S. Coast Guard, established three seismic-refraction profiles around the roughly triangular-shaped Island of Hawaii during August of 1964. These profiles were supplemented by recordings on the HVO seismic network of three high-energy explosions detonated by the U. S. Navy in February, April and June, 1965 on the island of Kahoolawe as part of the SAILOR HAT project. This paper gives a summary and an interpretation of these data, together with a re-evaluation of the data recorded on the HVO network from shots detonated in 1962 by the Scripps Institution of Oceanography off the northeast coast of Hawaii (Pollard and Eaton, 1964).

Travel-time curves presently being used for the routine location of earthquakes at HVO were established by Eaton (1962) (see also MacDonald and Eaton, 1964) from recordings of three earthquakes with magnitudes between 5.2 and 5.7 which occurred under Kilauea in 1955. These travel-time curves were interpreted in terms of a two-layer crust having a 3.9-km/sec layer 3.1 km thick over a 5.0-km/sec layer 9.4 km thick and an 8.25-km/sec upper mantle. On the basis of weak secondary arrivals, Eaton proposed an alternate, three-layer crust with the 5.0-km/sec layer reduced to a thickness of 8.1 km and a 6.8-km/sec layer 3.6 km thick forming the base of the crust.

Preliminary interpretation by Pollard and Eaton (1964) of data recorded from the two seismic-refraction profiles shot just off the northeast coast of Hawaii by the Scripps Institution of Oceanography in 1962 further substantiates the existence of a 6.8- to 7.0-km/sec layer at the base of the crust under Hawaii. The Scripps data also suggest that crustal thickness increases from 12 km near Hilo to 14 km under Kilauea and Mauna Loa.

In 1963 the Geological Survey established a seismic-refraction profile across the summit of Kilauea between Hilo and South Point. Ryall's interpretation of this data in 1968 generally supports the crustal structure reported by Pollard and Eaton (1964), but suggests shallow high-velocity material under the summit of Kilauea and a possible thinning of the crust from about 14 km between Hilo and the summit to as little as 10 km under the summit (Ryall and Bennett, 1968).

Additional seismic-refraction work defining the variations in crustal structure northwest of the Island of Hawaii includes a survey off the northeast coast of Maui by Shor and Pollard (1964), a survey near the Gardner Pinnacles (Shor, 1960), and several surveys on and near Oahu by the group at the Hawaiian Institute of Geophysics (Adams and Furumoto, 1965; Furumoto, Thompson and Woollard, 1965; Furumoto and Woollard, 1965).

Geologic Setting

The Hawaiian Islands are part of a 2600-km-long archipelago of basaltic shield volcanoes that rise from the crest of the northwest-southeast trending Hawaiian ridge. The islands tend to be progressively younger to the southeast along the chain, and Hawaii, the southeasternmost island in the chain, is both the youngest and largest of the islands. A moat-arch system parallels the northeastern flank of the Hawaiian ridge and bends part way around the island of Hawaii at the southeastern end of the ridge

(e.g., see Menard, 1964, p. 80). The ocean floor southwest of the ridge is marked by numerous seamounts.

The island of Hawaii is formed by the conjunction of five individual shield volcanoes (Figure 1). From north to south they are: (1) Kohala Mountain (altitude 1680 m), long dormant and the oldest volcano on Hawaii; (2) Mauna Kea (altitude 4,200 m) some activity following the last glacial epoch; (3) Hualalai (altitude 2,500 m), last active in 1801; (4) Mauna Loa (altitude 4,160 m), last active in 1950; and (5) Kilauea (altitude 1,240 m), presently the most active of the volcanoes and last active in July 1968.

On the younger volcanoes (Kilauea, Mauna Loa and Hualalai) eruptions issue either from the central caldera area or from two or three rift zones that radiate from the central areas. These rift zones are marked by fissures, grabens, cinder cones, spatter cones, and pit craters. On the older volcanoes (Mauna Kea and Kohala) eruptive vents tend to be scattered over the central areas of the shields, and the rift zones become less prominent but may still be recognized by lines of more numerous vents. Where exposed by deep erosion, the rift zones consist of a complex of numerous dikes of dense basalt (Wentworth and Jones, 1940).

A strong central gravity high is observed over the summits of all five volcanoes, and the rift zones are clearly marked by elongated gravity highs emanating from the summits (Kinoshita *et al*, 1963; Kinoshita, 1965).

Field Methods

The seismic-refraction profiles established along the three principal coasts of Hawaii in August 1964 were shot using fixed, on-shore recording positions and a moving, off-shore shotpoint. The U. S. Coast Guard Cutter CAPE SMALL, a 95-foot craft with a displacement of about 100 tons, served as shotpoint boat. Charges ranging from 300 to 400 pounds of Nitramon were fired at a depth of 15 meters from the CAPE SMALL at 10-km intervals along each of the three coasts. The firing depth of 15 m was determined to be the approximate depth at which the bubble from the detonated charge expanded and collapsed once before reaching the surface, thus minimizing the effect of bubble pulses. The positions of the shots were determined from magnetic bearing to several prominent landmarks on shore, and water depths under the shotpoints were measured by an electronic fathometer. All the shots were fired within 2 km of the shore, permitting short sightings at a wide range of angles. Allowing for drift between the time the charge was lowered into the water (the time when the depth measurements and bearing readings were made) and the time the shot was fired, the shotpoint locations are probably accurate to within ± 100 m. Timing of the shots to 0.01 sec was accomplished by electronically interrupting a radio-tone broadcast from the shooting boat at the shot instant.

The shots fired along a particular coastline were recorded by five seismic-refraction units spaced at approximately 25-km intervals along each coast and by the 13 short-period seismograph stations forming the permanent HVO seismic network.

The basic spread of each of the five refraction units was 2.5 km with six vertical seismometers (1.0-sec free period) spaced at 0.5-km intervals. Three types of seismic-refraction units were used to record the shots:

(1) Three long-range, 8-channel units of the type used by the U. S. Geological Survey for crustal studies within the continental United States. These units recorded the six vertical seismic channels and timing data on both magnetic tape and photo-

graphic paper plus two horizontal seismic channels on photographic paper. The units are described more fully by Warrick *et al* (1961).

(2) One low-frequency unit which recorded timing data and six seismic channels at two levels on photographic paper.

(3) One 12-channel unit using SIE TGA-2a seismic amplifiers in conjunction with a Honeywell magnetic-tape system. Normally this unit is set up to record from a 12-element 5- by 6-km L-shaped array on the summit of Kilauea, but for the seismic-refraction survey it was used as a mobile unit with the 12 channels used to record six seismic channels at two levels on both magnetic tape and photographic paper.

The radio-tone broadcast from the shooting boat and time signals from WWVH were recorded by the first type of refraction units described above. The low-frequency unit and the 12-channel unit recorded only WWVH. The shot-time tone break was clearly recorded by at least one refraction unit for each of the shots, and WWVH was usually clearly recorded by all of the units. Thus, with a few exceptions, arrivals from the shots could be timed on each of the refraction units to within 0.01 sec of WWVH.

Of the thirteen distinct recording positions occupied by the seismic-refraction units during the August 1964 shooting, eight were located in areas covered by U. S. Geological Survey $7\frac{1}{2}$-minute quadrangle maps. Locations of these units are accurate to within 10 m. The remaining five recording positions were located in areas covered by older, 15-minute quadrangle maps. Locations of these units are probably accurate to within 50 m.

Energy from the seismic-refraction explosions and the SAILOR HAT events was also recorded by most of the 13 short-period seismographs of the permanent HVO network. These short-period instruments have a free period of about 1.0 sec and peak magnifications of from 20,000 to 40,000 at a period of 0.2 sec. Locations of the short-period stations on Hawaii are shown on Figure 1 (also see Okamura, Koyanagi, Powers, 1965). The six stations around the summit of Kilauea are telemetered to the Observatory, where they are recorded on smoked-paper drums. The remaining eight stations are self contained and record on photographic paper. All of the short-period stations record with a chart speed of 1 mm/sec and timing on the short-period seisomograms is, in most cases, accurate to within 0.1 sec of WWVH time signal. To improve the time resolution on four of the Kilauea telemetered stations (Mauna Loa, West Pit, Ahua, and Makaopuhi) during the seismic-refraction program and the SAILOR HAT events, these stations were recorded on a Sanborn strip with a chart speed of 5 mm/sec. Timing on these four stations is probably accurate to within 0.05 sec.

On February 9, April 16 and June 19, 1965, the U. S. Navy detonated 500-ton charges of high explosives on the ground surface on the western point of Kahoolawe island as part of its SAILOR HAT program (Figure 2). The location to the nearest 0.01 sec of arc and shot times of the blasts to the nearest millisecond were provided by the U. S. Navy. The *P* waves generated by the blasts were clearly recorded on most of the short-period stations in the HVO seismic network and by two mobile recording units placed at different locations for each of the blasts (Figures 1 and 2).

For the February 9 event, the 12-channel unit described above recorded from the 5- by 6-km L-shaped stationing located just south of Kilauea caldera (B1 on Figure 1). For April 16 and June 19 events, the 12-channel unit recorded from a 3.0-km spread of six vertical seismometers located at two points along the Kona coast (B2 and B3 on Figure 1). In addition, the June 19 event was recorded by a two-channel mobile unit at the north end of the island of Hawaii on the flank of Kohala Mountain (P3 on Figure 1).

Data Reduction

Coastal Profiles. Travel-times were reduced to a datum of sea level by (1) subtracting travel times through rocks above sea level under the recording stations and (2) "re-

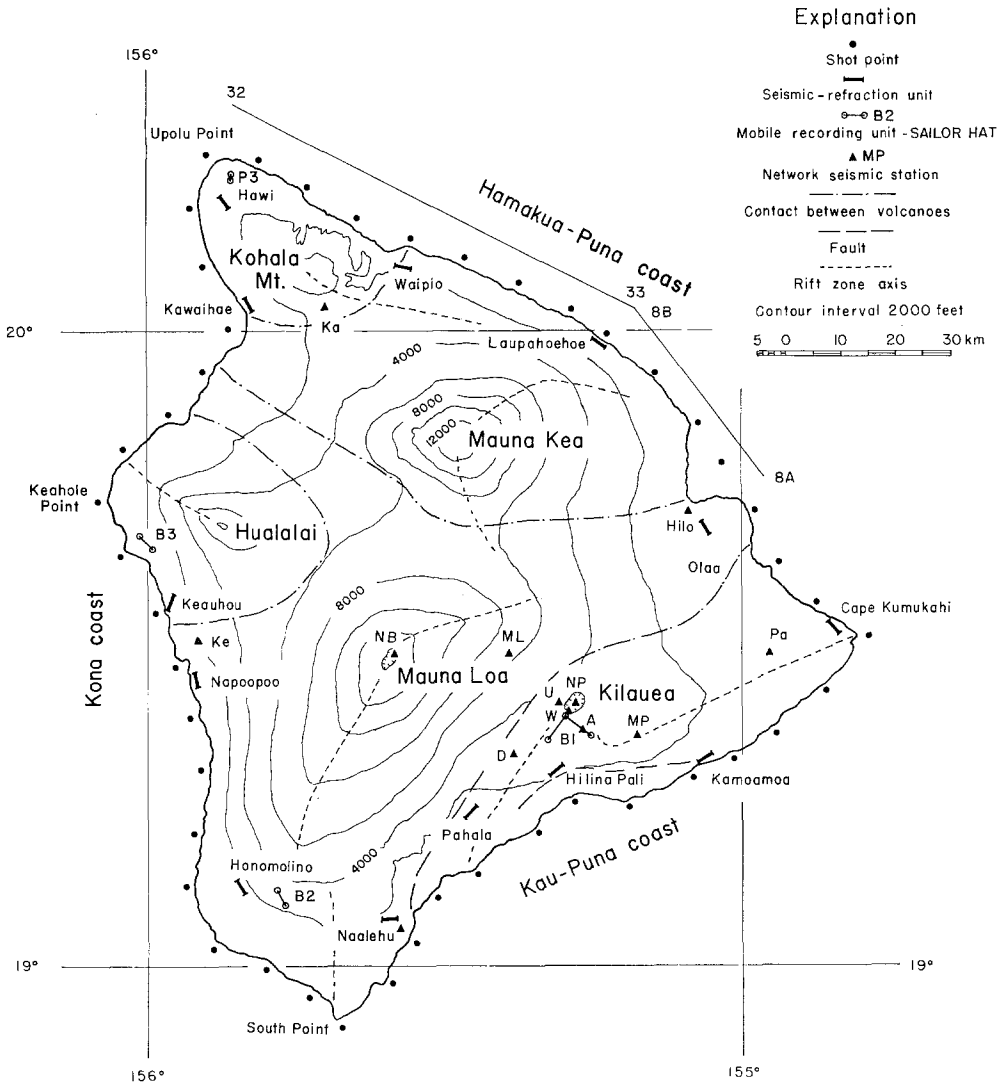

FIG. 1. Map of Hawaii showing locations of shotpoints, mobile recording units and permanent HVO seismograph stations. Map abbreviations for locations of seismograph stations referred to in text are as follows: A = Ahua, D = Desert, Hi = Hilo, Ka = Kamuela, Ke = Keanakakoi, ML = Mauna Loa, MP = Makaopuhi, Na = Nauleho, NB = North Bay, NP = North Pit, Pa = Pahoa, U = Uwekahuna, WP = West Pit. Lines 32–33 and 8A–8B are approximate locations of Scripps Institution of Oceanography seismic-refraction profiles shot in 1962.

placing" the water travel time between the shotpoints and the ocean bottom with that appropriate for near-surface rocks. Most corrections were 0.2 sec or less, but a few were as large as 0.5 sec. The *P*-wave velocities for near-surface rocks used in making these corrections were based on a composite plot of first arrivals recorded by the five refraction units in the distance range of 0 to 10 km. Because the 10-km spacing of the shotpoints is large with respect to distances required to define the near-surface structure

in adequate detail, the near-surface velocity distributions used to make the corrections can only be assumed to approximate an average for each coast.

The travel-time data from the profiles along each coast have been plotted with the shotpoints and recording positions interchanged to present the travel-time curves as if they had been generated by a fixed shotpoint and moving (or multiple) recording positions. Given reciprocity of travel times between shotpoints and recording positions, the only significant difference between this plot and a standard, fixed shotpoint

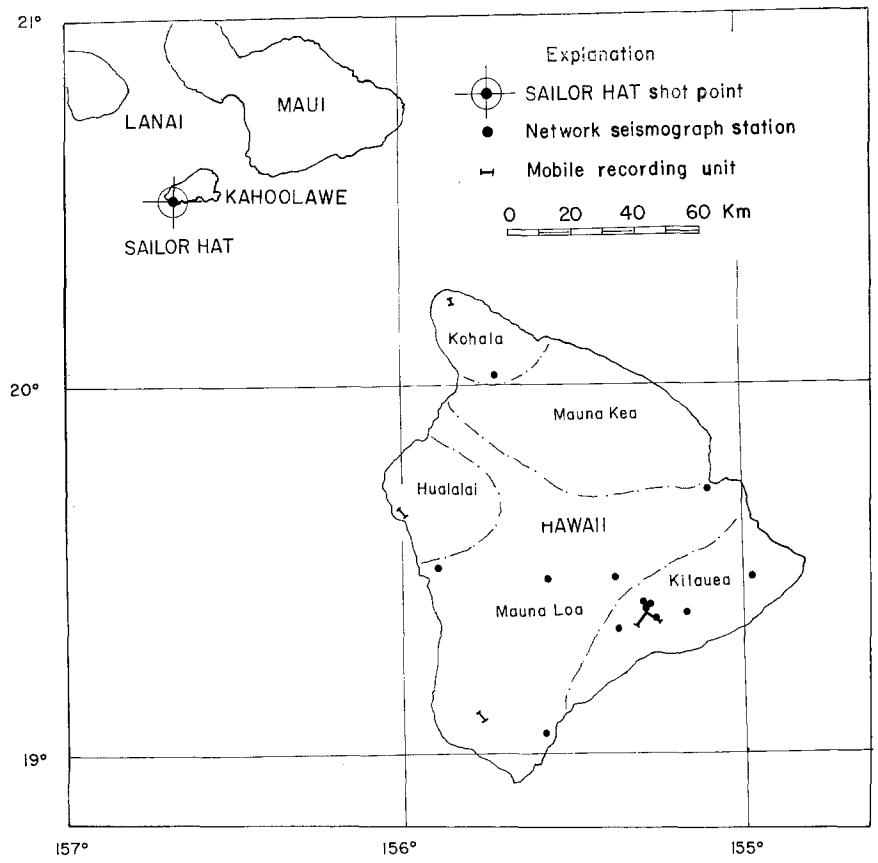

FIG. 2. Map showing location of SAILOR HAT shotpoint on Kahoolawe with respect to recording locations on Hawaii.

plot is that dipping structure under the fixed recording spread introduces a constant bias in the apparent velocity across the spread along a given travel-time segment rather than a variety of apparent velocities introduced by a moving spread across different structures.

First arrivals recorded on the five refraction units from the shots fired along each coast were initially picked from photographic monitor records. Playbacks were subsequently made from the magnetic tapes recorded by four of the units, and record sections were constructed from these playbacks. Final picks of secondary and weak first arrivals were made on the basis of phase correlations suggested by these record sections. All the arrivals plotted in the travel-time curves were read to the nearest 0.01 sec. The onsets of strong first arrivals are probably good to within ± 0.01 sec, but onsets of secondary arrivals and weak first arrivals may be uncertain by ± 0.1 sec.

Straight-line segments were visually fitted to the plotted first arrivals, and in some cases adjusted to include prominent secondary arrivals. The particular line segments drawn depend to an extent on interpretation, but in general, other line segments drawn to give a reasonable fit to the plotted arrivals would agree with the apparent velocity and intercept times of the line segments presented here within ± 0.1 km/sec and ± 0.2 sec respectively.

As can be seen on Figure 1, neither the shotpoints nor the recording locations along a given coast lie along a straight line. For convenience in plotting the travel-time curves along a given coast as one profile, the recording positions have been projected onto an average line drawn through the recording locations along each coast. The distances between recording locations in the profiles for each coast are these projected distances rather than true map distances. The plotted shotpoint-receiver distances, however, are true distances determined by the method described by Richter (1958). As a result, arrivals recorded from a given shot by any two receivers do not necessarily have the same abscissa along the profiles.

SAILOR HAT. First arrivals from the three SAILOR HAT events were read to the nearest 0.1 sec on records from the HVO seismic network and to the nearest 0.01 sec on monitor records from the 12-channel mobile array. The onset of the P phase (P_n at all stations on Hawaii) was impulsive on most of the stations for at least one of the shots; variations in first-motion quality were largely due to local noise conditions. For stations recording readable first motion from two or three of the SAILOR HAT events, each arrival time was picked and the average of these used for interpretation. The picked arrival times for all repeated stations, except Desert, are within ± 0.1 sec of the average time. The spread of picked arrival times from the Desert station is ± 0.2 sec; this larger spread is probably due to the fairly high noise level at Desert for the last two events. Because many of the stations recording the SAILOR HAT event were located inland and in areas of complicated or poorly known near-surface velocity structure, evelation corrections were not applied to the SAILOR HAT data.

HVO recordings of Scripps' shots. Seismic-refraction profiles shot off the northeast coast of Hawaii by Scripps Institution of Oceanography in 1962 generated P waves that were recorded on the HVO short-period seismic network. Information on size, location, time, depth, and distance above the sea floor of the explosions was made available by D. D. Pollard (personal communication, 1966). A preliminary interpretation of these data together with the reversed Scripps offshore profiles has been presented by Pollard and Eaton (1964).

The two profiles along which the Scripps shots were fired are shown in Figure 1. The shots were recorded with good timing on seven stations of the HVO seismic network (Hilo, Pahoa, Mauna Loa, Uwekahuna, North Pit, Ahua and Desert). First arrivals from the southeastern half of profile 32–33 were sharp and could be read to the nearest 0.1 sec on all of these stations; first arrivals from the larger shots along the northwestern half of profile 32–33 were clearly recorded on some stations but were lost in the background noise on others. In this paper we will consider only arrivals recorded at Hilo and Pahoa.

Arrival times from the Scripps shots were corrected for water depth but not for station elevation. However elevation corrections for the Hilo and Pahoa stations (20 m and 205 m above sea level, respectively, should be less than 0.05 sec. The travel-time segments used in this paper are those J. P. Eaton (personal communication, 1966) fitted by least squares to the time-distance values of the first arrivals. The average deviation of the observed arrival times from the least-square lines is less than 0.1 sec at each station.

Travel-Time Curves and Crustal Structure

Because the shot points and recording locations forming the coastal profiles do not lie along straight lines, none of the travel-time curves is truly reversed. In most cases attempts to interpret opposing or overlapping travel-time curves along a given coastal profile using standard, two-dimensional dipping layer techniques did not yield self consistent solutions. The implication is that variations in subsurface structure perpendicular to the profiles effect the differences in propogation paths for "reversed" and "overlapping" travel-time segments imposed by the shot point-receiver geometry.

These complications introduce an additional element of uncertainity in the interpretation and require some modification in the usual method of analysis of seismic refraction profiles. In this paper the following approach was taken with travel-time curves that could not be treated by a standard two-dimensional analysis:

(1) The P-wave velocity of a refracting horizon was established as a "best guess" from opposing travel-time segments in travel-time curves judged to be most nearly reversed. Depths to and dips on the horizon were then obtained by solving individual travel-time curves separately using the best guess P-wave velocity.

(2) In cases where this approach leads to a complex combination of solutions for shallow to intermediate crustal horizons between several travel-time curves, an average of these solutions was taken in computing depths to deeper crustal horizons of the M discontinuity.

(3) In cases where refracted arrivals from shallow to intermediate horizons were not reversed (even in a loose sense) the horizons were assumed to be horizontal.

(4) In all cases where travel time solutions were ambiguous, the known geology (primarily the locations of rift zones) was used as a guide to picking a plausible solution.

Thus the analysis of the coastal profiles presented in this paper is based more strongly on inductive reasoning than would be necessary if the geometry of the experiment were more favorable, and the resulting interpretation is not unique. Nevertheless, I feel that the interpretation represents the most plausible solution consistent with the measured travel time and the known geology.

Hamakua-Puna coast. The northeast coast (Hamakua Puna) of Hawaii is composed of the northeast flank of Kilauea between Cape Kumukahi and Olaa, a short section of Mauna Loa between Olaa and Hilo, and the flanks of Mauna Kea and Kohala Mountain between Hilo and Waipio and from Waipio to Upolo Point respectively (Figure 1). The travel-time curves recorded along this coast by four of the seismic-refraction units, together with their interpretation in terms of a crust section, are shown on Figure 3. (Because of mechanical problems, timing on the fifth unit, near Hilo, was lost for shots along the Hamakua coast.) Travel-time segments drawn through the plotted arrivals are summarized in Table 1.

From Figure 3 it is evident that, for shot-receiver distances larger than about 10 km, the apparent velocities of first arrivals recorded by the unit on the flank of Kilauea (Cape Kumukahi) are distinctly different from those recorded by units along the flanks of Kohala Mountain and Mauna Kea (Hawi, Waipio and Laupahoehoe). First arrivals at Cape Kumukahi define a 5.1-km/sec branch out to about 31 km and a 8.2-km/sec branch beyond to about 10 km, whereas first arrivals at the other units define single branches with apparent velocities between 6.2 and 7.6 km/sec from 9 km out to more than 100 km.

Beginning with the Cape Kumukahi travel-time curve, first arrivals from a shot 6.5 km northwest of the recording unit define the travel-time segment $T_1 = 0.60 + \Delta/3.3$. Assuming a travel-time segment $T_0 = 0.00 + \Delta/2.5$ for the surface layers, the near-

surface velocity structure north of Cape Kumukahi is given by a 2.5-km/sec layer 1.3 km thick over a 3.3-km/sec layer.

The 5.1-km/sec branch has a 1.35-sec intercept time, and if the layering along the northeast flank of Kilauea is essentially horizontal, the depth to the top of the 5.1-km/sec layer is about 2.3 km. The 8.2-km/sec first arrivals are interpreted as arrivals refracted from the M discontinuity (P_n). The intercept time of the P_n branch is 3.85 sec.

Two sets of secondary arrivals follow the 5.1-km/sec first arrivals by 1.2 and 1.6 sec from a shot 23 km northwest of Cape Kumukahi. The later of these arrivals falls

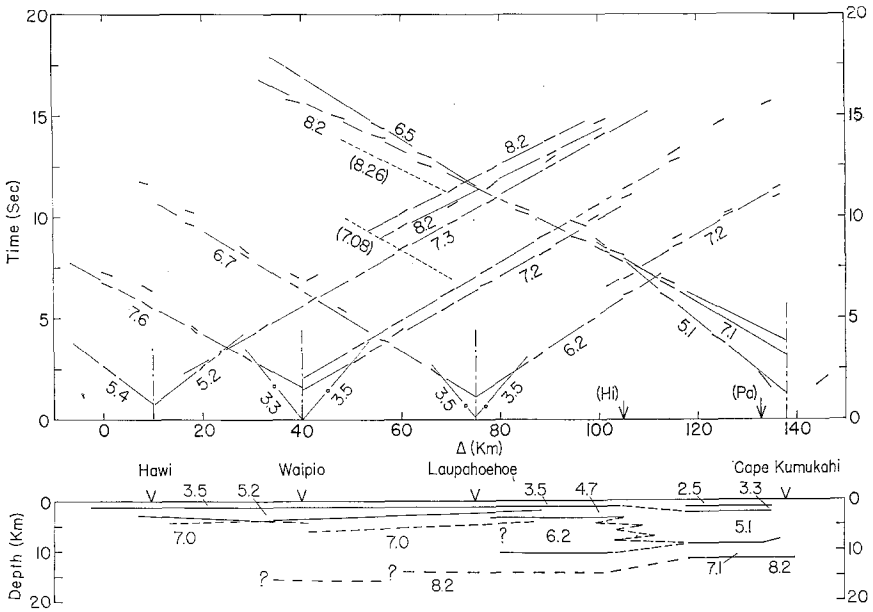

FIG. 3. Travel-time curves and crustal structure along the Hamakua coast. Numbers under the travel-time segments and in the crustal section are P-wave velocities in km/sec. (Hi) and (Pa) indicate the projected locations of the Hilo and Pahala seismograph stations in the plane of the profile. The dashed travel-time segments (7.80) and (8.26) were recorded at Hilo and Pahala respectively from the Scripps shots on profile 32–33. The missmatch in structure under Laupahoehoe is interpreted in terms of structural variations perpendicular to the profile; the shallow 7.0-km/sec horizons are further inland than the 6.2-km/sec horizon (see text). Dashed lines indicate uncertain structure. Δ, distance.

on the backward extension of the P_n branch and is interpreted as a reflection from the M discontinuity. The earlier arrival is probably a reflection from a deep crustal layer. On the basis of data yet to be discussed, it seems fairly certain that a 7.0- to 7.2-km/sec layer forms the base of the crust under Hawaii. A line with a 7.1-km/sec apparent velocity drawn through the earlier secondary arrival defines the travel-time segment $T_3 = 3.25 + \Delta/7.1$. Assuming again that the layering along the northeast flank of Kilauea is essentially horizontal, the depth to the top of a 7.1-km/sec layer is about 8.7 km, and the total crustal thickness is about 11.5 km (see Figure 3). This structure is in general agreement with the crustal structure just southwest of Hilo found by Ryall and Bennett (1968).

A composite plot of the near-surface arrivals recorded at Hawi, Waipio, and Laupahoehoe suggests that the average near-surface structure along the northeastern flanks of Kohala Mountain and Mauna Kea can be approximated by a 3.5-km/sec layer 1.5 km thick over a 5.2-km/sec layer.

Efforts to determine a P-wave velocity for the layer, or layers, refracting the 6.7- to 7.6-km/sec travel-time segments between Hawi and Laupahoehoe (and the 6.5-km/sec secondary arrivals recorded at Cape Kumukahi from shots northwest of Laupahoehoe) using standard reversed profile computations did not yield consistent results. However, the P-wave velocity of these layers is probably not very different from the average apparent velocities of the two longest, most nearly reversed travel-time seg-

TABLE 1

TRAVEL TIMES ALONG NORTHEAST COAST

Refraction Unit	Bearing of Shots from Unit	Travel-time Curves (sec)	Distance Interval Recorded (km)
Cape Kumukahi	Northwest	$T_0 = 0.00 + \Delta/2.5$ (assumed)	(0–3)
		$T_1 = 0.60 + \Delta/3.3$	3–6.5
		$T_2 = 1.35 + \Delta/5.1$	6.5–31
		$T_3 = 3.25 + \Delta/7.1$	23–25
		$T_4 = 3.85 + \Delta/8.2$	31–100
Hilo	No timing on Hilo records for Hamakua shots.		
Laupahoehoe	Northwest	$T_0 = 0.00 + \Delta/3.5$	0–7
		$T_1 = 0.75 + \Delta/5.2$ (assumed)	
		$T_2 = 1.15 + \Delta/6.7$	7–60
	Southeast	$T_0 = 0.00 + \Delta/3.5$	0–8
		$T_1 = 0.75 + \Delta/5.2$ (assumed)	
		$T_2 = 1.20 + \Delta/6.2$	8–32
		$T_2' = 2.80 + \Delta/7.2$	40–62
Waipio	Northwest	$T_0 = 0.00 + \Delta/3.3$	0–9
		$T_1 = 0.75 + \Delta/5.2$ (assumed)	
		$T_2 = 1.50 + \Delta/7.6$	10–41
	Southeast	$T_0 = 0.00 + \Delta/3.5$	0–9
		$T_1 = 0.75 + \Delta/5.2$ (assumed)	
		$T_2 = 2.00 + \Delta/7.2$	10–68
Hawi	Southeast	$T_0 = 0.00 + \Delta/3.2$ (assumed)	
		$T_1 = 0.75 + \Delta/5.2$	6–12
		$T_3 = 1.50 + \Delta/7.3$	12–92
		$T_4 = 3.25 + \Delta/8.2$	42–79
		$T_4' = 4.00 + \Delta/8.2$	

ments, or 7.0 km/sec (from the 7.3- and 6.7-km/sec segments southeast of Hawi and northwest of Laupahoehoe respectively). Solutions of the individual travel-time curves in terms of depth to and dip on the 7.0-km/sec layers do not coincide, but they do define a general trend in which the 7.0-km/sec horizon lies at depths between 2.5 and 5.0 km under Laupahoehoe, 3.5 to 6.0 km under Waipio, and 3.0 to 4.5 km under Hawi. These individual solutions are indicated in Figure 3. The differences between the individual solutions of the travel-times segments may be significant in that they suggest the degree of relief on the 7.0-km/sec layer normal to the profiles. Note that the 24 km long travel-time segment ($T = 1.97 + \Delta/7.08$) recorded at Hilo from the Scripps' shots along profile 32–33 (which will be discussed later) is consistent with a shallow 7.0-km/sec horizon along the northeast flank of Mauna Kea.

Surface geology together with the Bouguer gravity map of Hawaii (Kinoshita *et al*' 1963; Kinoshita, 1965) indicate that the southeast rift zone of Kohala Mountain extends under the northeast flank of Mauna Kea and parallels the coast 10- to 15- km inland. The gravity map also indicates that the east rift zone of Mauna Kea joins the extension of the Kohala rift zone near Laupahoehoe as shown in Figure 1. It is likely that the 6.7- to 7.6-km/sec travel-time segments along the northeast flank of Kohala Mountain and Mauna Kea have been refracted from an interface formed by the dense material composing the core of these rift zones. An analogous situation is found along the northwest Koolau rift zone on Oahu. A large, elongated gravity high coincides with the axis of the Koolau rift zone (Woollard, 1951), and a recent seismic-refraction profile established along the northeast edge of the Koolau rift zone suggest that material with a P-wave velocity of 7.0 km/sec or greater is only 4 to 5 km deep under the rift zone (Furumoto *et al*, 1965).

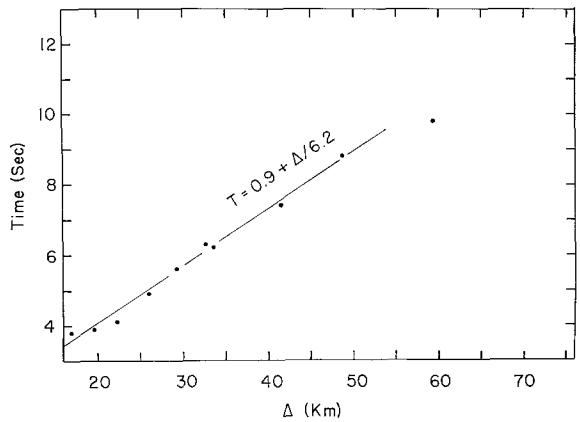

FIG. 4. Travel-time curve of first arrival recorded by the Kamuela seismograph stations from shots along the Hamakua coast. Δ, distance.

One should bear in mind that the refracting boundary of the rift zone may dip fairly steeply away from its axis (as suggested by the gravity field), and thus that, although the perpendicular distance from a dipping refracting horizon to the surface may be approximately as shown in Figure 3, the depth to the horizon vertically beneath the profile may be significantly larger than shown.

The permanent HVO seismograph station at Kamuela (Ka) is located about 5 km west of the maximum of the gravity high associated with the Kohala rift zone (Figure 1) and is thus near the line along which the material of the rift zone most closely approaches the surface. Figure 4 is standard time-distance plot of the first arrivals recorded by the Kamuela station from the shots fired along the northeast flanks of Kohala Mountain and Mauna Kea. These arrivals define a travel-time segment $T = 0.90 + \Delta/6.2$. Assuming that the near-surface velocity at Kamuela is about the same as along the coast (a 3.5-km/sec layer 1.5 km thick over a 5.2-km/sec layer) and that the observed first arrivals are refracted along the 7.0-km/sec interface of the rift zone core, the 7.0-km/sec layer is about 2.0 km deep under Kamuela and dips about 9° toward the coast (the northeast). If this dip is extrapolated to the coast, the depth of the 7.0-km/sec layer under the seismic-refraction profiles is about 7.0 km. The Kamuela travel-time curve is not reversed, and of course other interpretations are possible. One could assume, for example, that the apparent velocity of the travel-time curve repre-

sents the true velocity between Kamuela and the coast, and that this velocity is the result of vertical, high-velocity dikes (7.0 km/sec) interspersed with low-velocity flows (5.1 km/sec). In this case, the depth to a 6.0-km/sec "layer" would be about 2.3 km under Kamuela.

The seismic-refraction data yield an ambiguous picture for crustal structure beneath the shallow 7.0-km/sec horizon along the flanks of Kohala Mountain and Mauna Kea. The 6.7- to 7.6-km/sec travel-time segments recorded by units on the flanks of Kohala Mountain and Mauna Kea are defined by first arrivals out to maximum recording distances (~100 km); thus evidence for the deeper structure must come from secondary

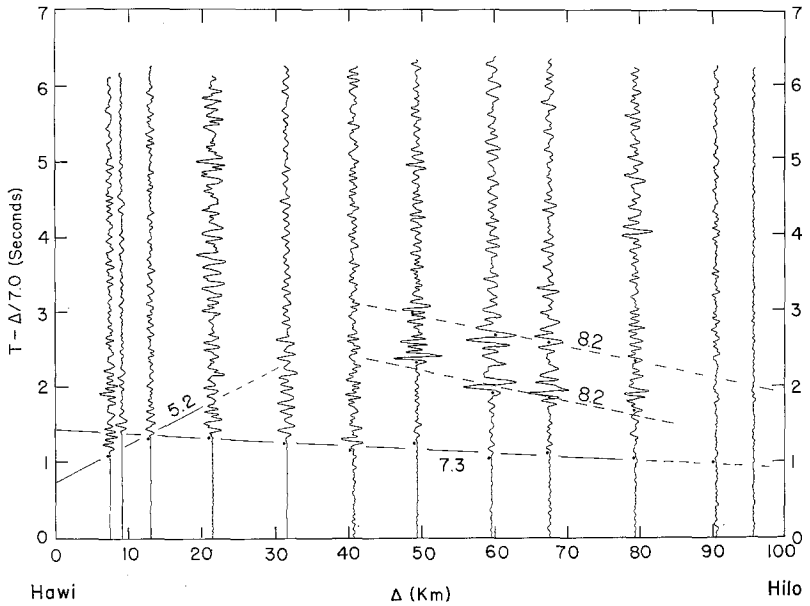

FIG. 5. Record section of arrivals recorded at Hawi from shots to the southeast along the Hamakua coast. Each plotted trace represents the output of one of six vertical seismic channels recorded by the refraction unit for each of the 12 shots. Lines drawn through secondary arrivals pass through positions picks (black dots) occupy when adjusted according to first arrival delays about the 7.3 km/sec line. Δ, distance.

arrivals on these travel-time curves and from the P_n arrivals recorded at Cape Kumukahi from shots along the northeast coast of Mauna Kea.

Two prominent sets of secondary arrivals follow the 7.3-km/sec first arrivals recorded at Hawi from shots 49 to 79 km to the southeast (Figures 3 and 5). A line drawn through the first large peak of the earliest set of secondary arrivals on each trace (corrected for near-surface delays according to the scatter in first arrivals about the 7.3-km/sec line) has the equation $T_4 = 3.2 + \Delta/8.2$. A line through the later set of arrivals similarly corrected for near-surface delays has the equation $T_4' = 4.0 + \Delta/8.3$.

The travel times and amplitudes of both sets of secondary arrivals are appropriate for reflections from the M discontinuity (P_MP) beyond the critical angle, where the distance at which the large-amplitude secondary arrivals are first observed is the critical distance (between 41 and 49 km on Figure 5). However, the nearly constant difference in arrival time (1.8 sec) and the marked similarity in character of the largest peak-trough pair between the two sets of arrivals suggests that the later set may be a multiple reflection of the earlier set and hence that the earlier set is P_MP.

If this is the case, the "intercept time" (3.2 sec) of the earlier set of arrivals requires that the P_n delay time be about 0.3 sec less under the flanks of Kohala Mountain and Mauna Kea than under the flanks of Kilauea and at least the southeastern section of Mauna Kea as indicated by the 3.85-sec intercept time of the Cape Kumukahi P_n branch. The subsurface "overlap" of the Cape Kumukahi P_n rays and the Hawi P_MP rays on the M discontinuity is small (less than 10 km under a region about 10 km northwest of Laupahoehoe), but the emerging rays do overlap through a broad section of the crust between Waipio and Laupahoehoe. Thus, if the smaller P_n delay suggested by the Hawi P_MP events is due to a higher average crustal velocity (as is possible in view of the shallow high velocity horizon in this area), the P_n arrivals beyond Laupahoehoe on the Cape Kumukahi branch should be about 0.3 sec earlier than observed. It is, of course, possible that the true onset of P_n on these records is lost in the noise and is earlier than picked.

One could, on the other hand, pick the later set of secondary arrivals as P_MP and interpret the earlier set of arrivals as a reflection from a steeply dipping layer somewhere within the crust (possibly associated with the complicated structure of the nearby rift zones?). The "intercept time" of these later arrivals (4.0 sec) is similar to that of Cape Kumukahi P_n branch (3.85 sec) and this avoids the problem of P_n delay differences through the Waipio to Laupahoehoe section of the crust.

To estimate depths to the M-discontinuity from the Hawi secondary arrivals, the individual solutions for the 7.0-km/sec horizon were replaced by an average horizontal 7.0 km/sec horizon. The results are as follows:

(1) If the earlier secondary arrivals are P_MP, the 7.0-km/sec layer is about 11 km thick, giving a total crustal thickness of about 16 km. The critical distance for this model is 42.5 km, just beyond the minimum distance admitted by the data (Figure 5). If an additional 5.2-km/sec layer lies between the 7.0-km/sec layer and a 7.1-km/sec layer at the base of the crust (i.e., if the shallow 7.0-km/sec horizon is a sill), the crustal thickness may be as little as 12 km and the critical distance should occur somewhere between 25 and 40 km from Hawi.

(2) If the later secondary arrivals are P_MP, the 7.0-km/sec layer is about 15 km thick, giving a total crustal thickness of about 20 km. Of course the total crustal thickness can also be reduced in this case if the shallow 7.0-km/sec horizon is regarded as a sill underlain by low-velocity material.

Note that the 5.1-km/sec layer between Hawi and Laupahoehoe is based only on arrivals recorded at Hawi. If this layer is omitted in the analysis of the Hamakua coast, the computed depths to the deeper horizons are decreased by somewhat less than one km.

The Scripps Institution of Oceanography profiles 32–33 (Figure 1), shot 5 to 10 km off the Hamakua coast, provide independent data regarding crustal structure along the northeast flanks of Kohala Mountain and Mauna Kea. D. D. Pollard (personal communication, 1968) interprets these data as indicating that the crust under these profiles is only 11 to 12 km thick. On this basis, a thick crust (i.e., 20 km) directly under the coast would require a surprisingly large dip on the M discontinuity. Although the data do not necessarily preclude such a situation, it seems reasonable to accept the interpretation which treats the earlier secondary arrivals as P_MP, the later arrivals as multiple reflection, and gives crustal thicknesses between 12 to 15 km as most plausible.

The travel-time curve recorded at Laupahoehoe from shots to the southeast is transitional between the travel-time curves along the flanks of Mauna Kea and Kohala Mountain and the travel-time curve from Cape Kumukahi to the northwest. The near-

surface velocity distribution for the travel-time curve southeast of Laupahoehoe is based on arrivals recorded at the Hilo seismograph station from shots detonated by Scripps along profile 32–33 (see below). Arrivals from shots fired between 8 and 32 km southeast of Laupahoehoe define the travel-time segment $T_2 = 1.20 + \Delta/6.2$, and arrivals from shots fired between about 40 and 62 km southeast define the travel-time segment $T_2' = 2.80 + \Delta/7.2$. The first arrivals defining the 7.2-km/sec segment are 0.7 to 1.0 sec late with respect to the projected trend of the 6.2-km/sec segment beyond 30 km. This difference can be explained either as a discontinuity in the layer refracting the 6.2-km/sec arrivals or as failure to identify 6.2-km/sec events as first arrivals beyond 30 km. The latter seems unlikely, however, since the noise level for the Laupahoehoe records is virtually the same for shots over the entire distance range.

The Scripps profile 8A–8B is parallel to, and about the same length as, the Laupahoehoe 6.2-km/sec travel-time segment (Figure 1). This reversed Scripps profile defines a 6.2-km/sec layer at a depth of about 3 to 4 km (D. D. Pollard, personal communication, 1968). Since the two profiles are separated by only about 5 km it seems reasonable to regard the 6.2-km/sec travel-time segment from Laupahoehoe as having been refracted from this same 6.2-km/sec layer. The solution of the 6.2-km/sec Laupahoehoe travel-time segment using the near-surface velocity distribution assumed above yields a depth to the 6.2-km/sec layer of 3.5 km—virtually the same as that for the Scripps profile 8A–8B.

The apparent disagreement between the overlapping Wapio and Hawi 7.3- and 7.2-km/sec branches southeast of Laupahoehoe and the 6.2-km/sec branch from Laupahoehoe to the southeast may be explained in terms of lateral variations in structure. Propagation paths between shots southeast of Laupahoehoe and the Waipio and Hawi recording positions pass further inland (and closer to the dense central core and east rift zone of Mauna Kea) than propagation paths between these shot points and the Laupahoehoe recording position. The structure shown in Figure 3 is intended to illustrate this situation in that the 7.0 km/sec horizons southeast of Laupahoehoe are supposed to be further inland than the 6.2 km/sec horizon.

The 7.2-km/sec travel-time segment southeast of Laupahoehoe was generated from shots fired along the northeast flank of Kilauea. One explanation of the arrival times of these events at Laupahoehoe involves ray paths traveling down through the 2.5-, 3.3-, and 5.1-km/sec layers under Kilauea and thence as a head wave along a 7.2-km/sec layer 10.4 km deep. This model requires that the 7.1-km/sec layer under Kilauea increase in depth from 8.7 to 10.4 km and in velocity from 7.1 to 7.2 km/sec somewhere in the vicinity of Hilo (see Figure 3).

Travel-time curves recorded at Hilo and Pahoa from the Scripps shots along the southeastern half of profile 32–33 are plotted on Figure 6. Both of these travel-time curves have been projected into the plane of Figure 3 for comparison with the August 1964 data. The travel-time segment from arrivals recorded at Hilo from the Scripps shots covers a 24-km segment between Laupahoehoe and Waipio. The apparent velocity (7.08 km/sec) and intercept time (1.97 sec) of this travel-time segment compare with the "overlapping" and "reversed" 6.7- and 7.0-km/sec branches recorded at Laupahoehoe and Waipio. Thus it seems likely that the arrivals from the Scripps shots recorded at Hilo have been refracted along the shallow 7.0-km/sec horizon associated with the Mauna Kea rift zone. Two prominent sets of secondary arrivals recorded at Hilo define the travel-time segments $T = 0.45 + \Delta/4.7$ and $T = 0.00 + \Delta/3.7$ (Figure 6). These travel-time segments suggest that the shallow structure northwest of Hilo is

composed of a 3.5-km/sec layer 1.2 km thick over a 4.7-km/sec layer. If the 7.08-km/sec travel-time segment from Hilo is treated as being roughly reversed by the 7.2-km/sec segment southeast of Waipio, the 7.0-km/sec horizon lies at a depth of about 5 km under Laupahoehoe and 6 km under Waipio. This is about 2 km deeper than determined from the Hawi 7.4-km/sec travel-time segment, but again, the profiles are not truly reversed, and this difference is probably an indication of relief on the 7.0-km/sec layer.

If the Pahoa travel-time curve from the Scripps shots (Figure 6) is projected into the plane of Figure 3, the Pahoa station will fall about 5 km northwest of Cape Kumukahi and the travel-time segment will span a 20-km interval between Waipio and Laupahoehoe (Figure 3). The 8.26-km/sec travel-time segment recorded at Pahoa closely agrees with the 8.2-km/sec P_n travel-time segment of the "overlapping" Cape Kumukahi

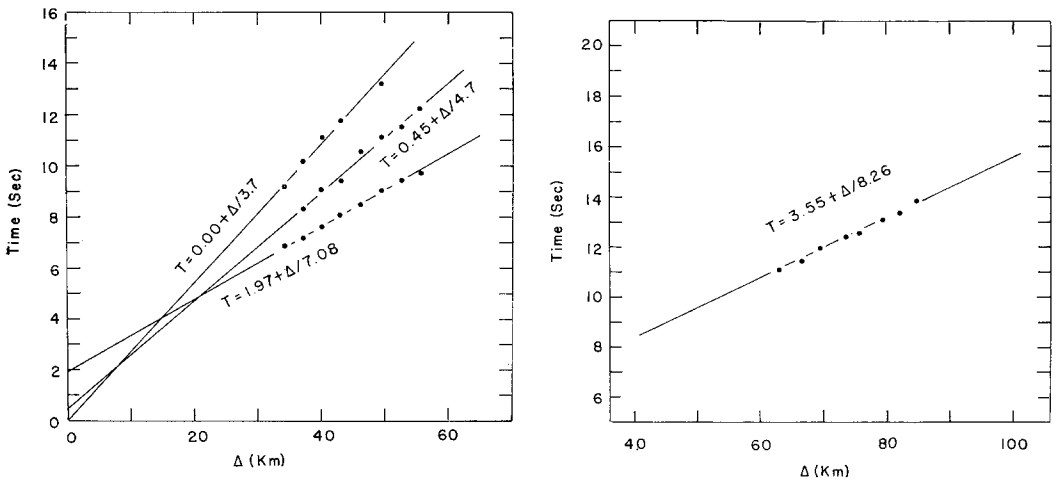

FIG. 6. Travel-time curves of arrivals recorded at Hilo (left) and Pahoa (right) from shots along Scripps' profile 32–33. Δ, distance.

data. The 3.55-sec intercept time of the Pahoa P_n segment, however, is 0.3 sec less than that of the Cape Kumukahi P_n segment. If this difference in intercept times is distributed equally as a smaller vertical P_n travel time (1.77 sec) under both Pahoa and the Scripps shotpoints than under Cape Kumukahi and the shotpoints just off the Mauna Kea coast (1.92 sec), the smaller P_n intercept time at Pahoa may be attributed to a lesser depth to the 7.2-km/sec layer under Pahoa—6.7 km instead of 8.7 km at Cape Kumukahi—and either a thinner crust or a higher average crustal velocity under the Scripps shotpoint than under the shotpoints just off the Mauna Kea coast.

Kona coast. The Kona, or west, coast of Hawaii is composed of the west flanks of Kohala Mountain, Hualalai, and Mauna Loa (Figure 1). The travel-time curves recorded along this coast by the five seismic-refraction units together with their interpretation in terms of crustal structure are shown in Figure 7. Travel-time segments drawn through the arrivals on Figure 7 are summarized in Table 2.

A composite plot of first arrivals from shots 10 km or less from units along the flanks of Mauna Loa and Hualalai (Keauhou, Napoopoo and Kawaihae) suggests that the average near-surface travel-time segments can be approximated by $T_0 = 0.00 + \Delta/2.5$ and $T_1 = 0.61 + \Delta/4.7$. First arrivals from shots 13 km or less from units along the flanks of Kohala Mountain (Kawaihae and Hawi) define the travel time segments $T_0 =$

$0.00 + \Delta/3.4$ and $T_1 = 0.20 + \Delta/4.1$ respectively, and for this analysis, it is assumed that the near-surface P-wave velocity along the flank of Kohala Mountain is close to the average apparent velocity of these two travel-time segments, or 3.7 km/sec. Thus, as shown on Figure 7, the near-surface velocity structure along the flanks of Mauna Loa and Hualalai is taken to be a 2.5-km/sec layer 0.7 km thick over a 4.7-km/sec layer and along the flank of Kohala Mountain a 3.7-km/sec layer.

First arrivals recorded by all five units for shot-receiver distances between 10 and 54 km define travel-time segments with apparent velocities between 5.6 and 6.3 km/sec and with intercept times between 1.4 and 1.8 sec (Table 2). The longest and most clearly defined of these segments has a velocity of 6.0 km/sec recorded at Honomalino from shots between 30 and 52 km north. Taking 6.0 km/sec to be the average P-wave

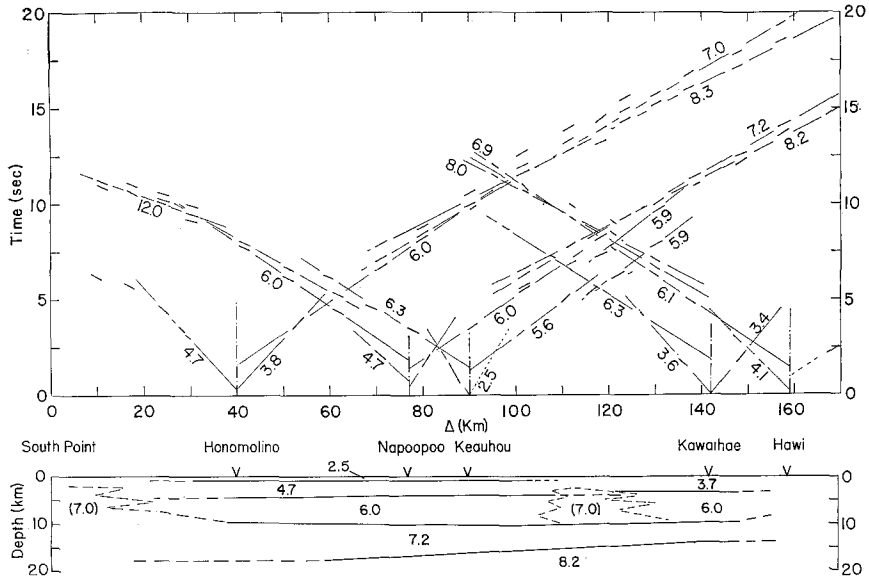

FIG. 7. Travel-time curves and crustal structure along the Kona coast. Dashed lines and parenthetic numbers indicate uncertain structure and P-wave velocity respectively. Δ, distance.

velocity of the horizon refracting the 5.6- to 6.3-km/sec arrivals and using the near-surface velocity distribution outlined above, the depth to the top of the 6.0-km/sec layer is about 4.0 km under Mauna Loa and Hualalai and about 3.3 km under Kohala Mountain.

The travel-time curves recorded at both Napoopoo and Keauhou from shots to the north show discontinuities about halfway between Keauhou and Kawaihae (110 km on the ordinate on Figure 7). In both cases the arrivals north of 110 km are advanced with respect to those south of 110 km by about 0.5 sec. This travel-time discontinuity occurs between the Hualalai rift zone and the northern contact between Hualalai and the Mauna Loa flows. The details of the structure in this area are complicated; the apparent velocities of the "overlapping" travel-time curves do not agree (6.0 and 5.6 km/sec from Napoopoo and Keauhou and 6.3 and 6.1 km/sec for Kawaihae and Hawi), and the discontinuities in the Keauhou and Napoopoo travel-time curves apparently are not reversed in the Hawi and Kawaihae travel-time curves.

Jerry Eaton (personal communication, 1966) suggests that these observed travel times might be expected, since the energy on both the Hawi and Kawaihae lines dies

out near Keahole Point at the west tip of Hualalai, whereas the discontinuities on the Keauhou and Napoopoo lines occur where the lines of shots swing around Keahole Point. The energy from shots to the north of Keahole Point travels along paths that

TABLE 2

TRAVEL TIMES ALONG THE KONA COAST

Refraction Unit	Bearing of Shots from Unit	Travel-time Curves	Distance Interval Recorded (km)
Honomalino	North	$T_0 = 0.00 + \Delta/2.5$ (assumed)	(0–15)
		$T_1 = 0.50 + \Delta/4.7$ (assumed)	
		$T_2 = 1.60 + \Delta/6.0$	15–52
		$T_3 = 2.75 + \Delta/7.0$	52–64
		$T_4 = 4.15 + \Delta/8.3$	64–118
	South	$T_1 = 0.30 + \Delta/4.7$	0–18
		$T_2 = 4.15 + \Delta/14.0$	18–32
Napoopoo	North	$T_0 = 0.50 + \Delta/2.8$	0–5
		$T_1 = 0.50 + \Delta/4.7$ (assumed)	
		$T_2 = 1.40 + \Delta/6.0$	5–50
		$T_3 = 2.75 + \Delta/7.2$	24–83
		$T_4 = 3.57 + \Delta/8.2$	50–83
	South	$T_1 = 0.75 + \Delta/4.7$	0–8
		$T_2 = 1.80 + \Delta/7.0$	8–45
		$T_3 = ? + \Delta/18$	45–68
Keauhou	North	$T_0 = 0.00 + \Delta/2.5$ (assumed)	(0–10)
		$T_1 = 0.50 + \Delta/4.7$ (assumed)	
		$T_2 = 1.25 = \Delta/5.6$	10–25
		$T_2' = 0.90 + \Delta/5.9$	25–42
	South	$T_0 = 0.00 + \Delta/2.5$	0–5
		$T_1 = 0.50 + \Delta/4.7$ (assumed)	
		$T_2 = 1.45 + \Delta/6.3$	11–31
Kawaihae	North	$T_0 = 0.00 + \Delta/3.4$	0–8
	South	$T_0 = 0.00 + \Delta/3.6$	0–7
		$T_1 = 0.60 + \Delta/4.7$ (assumed)	
		$T_2 = 1.80 + \Delta/6.3$	14–45
Hawi	South	$T_1 = 0.20 + \Delta/4.1$	0–13
		$T_2 = 1.4 + \Delta/6.1$	20–47
		$T_3 = 2.50 + \Delta/6.9$	28–64
		$T_4 = 3.40 + \Delta/8.0$	56–64

pass progressively closer to the center of the Hualalai structure on their way to Keauhou and Napoopoo than energy from shots south of the point. The early arrivals on the Keauhou and Napoopoo travel-time curves from shots north of Keahole Point may well be due to high-velocity material (7.0 km/sec) in the crust associated with the dense central core and west rift zone of Hualalai.

First arrivals beyond the 6.0- and 5.9-km/sec travel-time segments north of Honomalino and Napoopoo define the travel-time segments $T_3 = 4.15 + \Delta/8.3$ and $T_3 =$

3.57 + Δ/8.2, respectively. First arrivals from between 57 and 64 km south of Hawi supported by secondary arrivals between 28 and 48 km south of Hawi, define the travel-time segment $T_3 = 3.40 + \Delta/8.0$. These first arrivals are interpreted as P_n refractions from the M discontinuity and the secondary arrivals are interpreted as reflections from the M discontinuity (P_MP).

On the Honomalino travel-time curve, two sets of strong secondary arrivals follow the 6.0-km/sec first arrivals by 0.5 and 1.2 sec at 30 km and approach the 6.0-km/sec travel-time segment at about 60 km (the approximate P_n crossover distance). Similar secondary arrivals were recorded between 20 and 50 km north of Napoopoo and between 30 to 60 km south of Hawi. The earlier set of secondary arrivals line up with secondary arrivals beyond 50 to 60 km from the recording units and define travel-time segments $T_2 = 2.75 + \Delta/7.0$ (Honomalino), $T_2 = 2.75 + \Delta/7.2$ (Napoopoo), and $T_2 = 2.50 + \Delta/6.9$ (Hawi). The secondary arrivals at shot-receiver distances less than the P_n crossover distance are regarded as reflections from a 7.2-km/sec layer deep in the

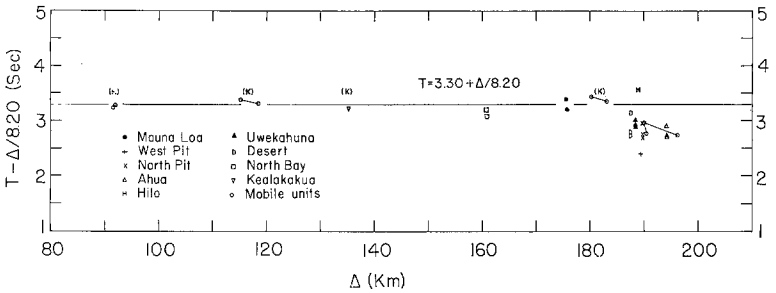

FIG. 8. Reduced travel times of first arrivals recorded on Hawaii from the three SAILOR HAT events detonated on Kahoolawe. (K) indicates recording positions along the Kona coast. Δ, distance.

crust, and the secondary arrivals beyond the P_n crossover distance are regarded as reflections from the M discontinuity. Although the T_2 travel-time segments are defined by two sets of reflections, they can be regarded as the approximate travel-time segments of arrivals refracted from the top of a 7.2-km/sec layer about 10 km deep.

The later set of secondary arrivals observed at shot-receiver distances less than the P_n crossover distance fall near the backward extension of the P_n travel-time segments and are interpreted as reflections from the M discontinuity (P_MP).

Additional evidence for the upper mantle (P_n) velocity under the west side of Hawaii is provided by recordings of the SAILOR HAT event at stations along the Kona coast. Figure 8 is a plot of the first arrivals from the three shots of the SAILOR HAT series recorded by stations on Hawaii with the ordinate reduced to $T - \Delta/8.2$ sec. First arrivals recorded by stations along the Kona coast (those arrivals marked (K) on Figure 8) scatter about the line segment $T = 3.30 + \Delta/8.2$ within ±0.1 sec.

The P_n travel-time segment defined by the Kona recordings of the SAILOR HAT events extends south-southwest from Kahoolawe and approximately reverses the P_n travel-time segment extending north from Honomalino. These two approximately reversed P_n travel-time segments suggest that the P_n velocity in the vicinity of the Kona coast is between 8.2 and 8.3 km/sec.

Intercept times of the P_n travel-time segments from Hawi and Napoopoo defined by shots along the Kona coast are 3.40 and 3.50 sec, respectively (Table 2). Assuming that the average P_n delay time along the central section of the Kona coast is approximately

half the average of these intercept times, or 1.72 sec, and neglecting a possible small dip on the M discontinuity, the 3.30 sec intercept time of the SAILOR HAT P_n segment suggests that the P_n delay time under the Kahoolawe shotpoint is about 1.58 sec.

A structure consistent with the travel-time curves for arrivals refracted from the top of the 7.2-km/sec layer is shown on Figure 7. The top of the 7.2-km/sec layer lies at a depth of about 10 km between Honomalino and Hawi. The P_n travel-time segments suggests that the depth to the M discontinuity decreases from about 18 km under Honomalino to about 14 km under Kawaihae and Hawi, and thus that the 7.2-km/sec layer decreases in thickness from about 7 km under Honomalino to about 4 km under Kawaihae and Hawi.

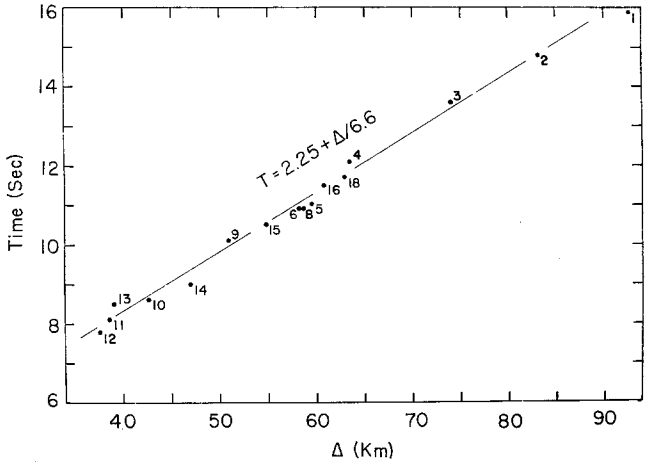

FIG. 9. Travel-time curve and first arrivals recorded at North Bay (Mauna Loa summit) from shots along the Kona coast. Δ, distance.

First arrivals recorded beyond 15 and 45 km south of Honomalino and Napoopoo respectively define travel-time segments with apparent velocities from 12- to 18-km/sec. The shots generating these arrivals were fired along the southwestern flank of the south rift zone of Mauna Loa (see Figure 1). Because no reasonable crustal materials have P-wave velocities much above 7.0-km/sec, these arrivals must be explained in terms of structure. A likely explanation is that the high-velocity arrivals have been propagated up dip along a horizon with a P-wave velocity near 7.0-km/sec from the top of the 7.2-km/sec layer to within a few kilometers of the surface near the axis of the rift zone. A possible distribution of this 7.0-km/sec material is suggested on Figure 7. Geologically this material probably represents a series of dense basaltic dikes and sills forming the core of the south rift zone of Mauna Loa.

The short-period seismograph located on the summit of Mauna Loa (NB on Figure 1) recorded clear first arrivals from most of the shots fired along the Kona coast. As can be seen on Figure 9, the first arrivals from all of the shots recorded fall within ± 0.3 sec of the line segment $T = 2.25 + \Delta/6.6$; this is somewhat surprising in view of the wide range of receiver-shotpoint aximuths.

A detailed interpretation of the Mauna Loa summit travel-time curve from the Kona shots is not justified because of the lack of control on the propagation paths over the wide range of aximuths. One can imagine, however, that the dense material associated with the cores and south rift zones of both Hualalai and Mauna Loa form a distribution of high-velocity material (7.0-km/sec ?) in the crust resulting in the ob-

served travel times. On the basis of the observed travel times, this high-velocity material might be described in broad terms as a 7.0-km/sec horizon dipping away from the summit of Mauna Loa at azimuths between N20°E and S10°E. If, for example, the Mauna Loa summit travel-time curve is treated as a single, dipping-layer seismic-refraction problem, and if the P-wave velocities of the refracting horizon and the overlying layer are assumed to be 7.0 and 4.7 km/sec, respectively, then the 7.0-km/sec layer is about 7 km deep (3 km below sea level) 6 to 8 km west of the summitt and dips away from the summit area at about 8° at azimuths west of a north-south line. According to this greatly simplified geometry, the 7.0-km/sec layer should inter-

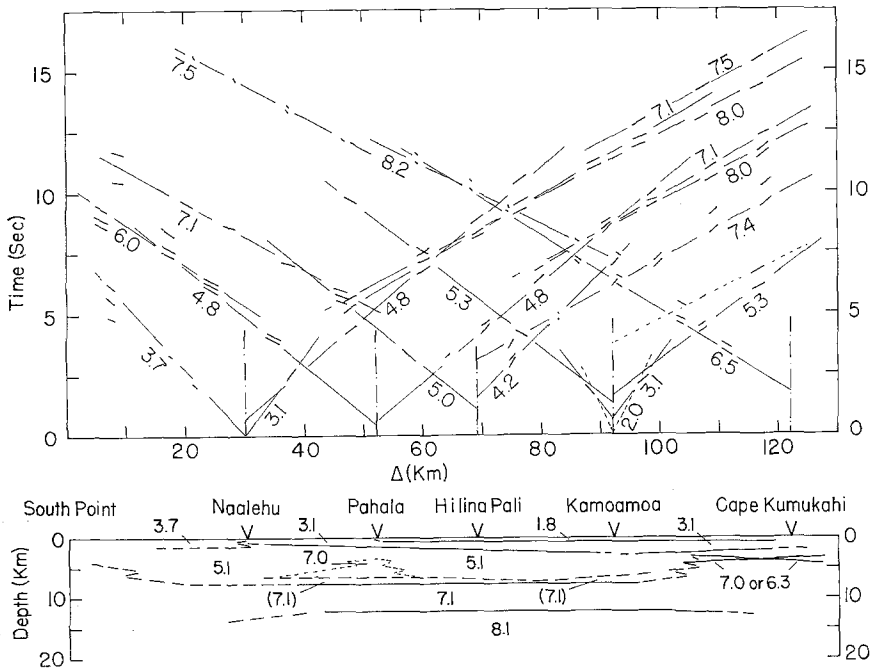

FIG. 10. Travel-time curves and crustal structure along Kau-Puna coast. Heavy dashed lines and parenthetic velocities indicate structure from the Hilina Pali refraction unit, which is somewhat behind, or inland from, the plane of the profile. Dashed structure under Pahala indicates approximate position of southwest rift zone core. Two possible solutions are given for the shallow, high-velocity horizon of the east rift zone. Δ, distance.

sect the profile along the Kona coast at depths from 8 to 10 km—or approximately the depth of the top of the 7.2-km/sec layer determined from the coastal profiles.

Kau-Puna coast. The southwesternmost 30 km of the Kau-Puna, or southeast coast of Hawaii, is composed of the flank of the south rift zone of Mauna Loa; the remainder of the coast northeast to Cape Kumukahi follows the southeast flank of Kilauea (Figure 1). The travel-time curves recorded by the five seismic-refraction units from shots fired along the Kau-Puna coast, together with their interpretation in terms of crustal structure, are shown on Figure 10. The travel-time segments drawn through the arrivals are summarized in Table 3.

First arrivals from shots between 3 and 6 km on either side of the recording unit located near Kamoamoa defined travel-time segments $T_0 = 0.70 + \Delta/3.1$. A line drawn through the origin and the first arrival recorded at 3 km gives the assumed travel-time segment $T_0 = 0.00 + \Delta/1.8$. The structure suggested by these two travel-time segments is a 1.8-km/sec layer 0.7 km thick over a 3.1-km/sec layer, and in the

absence of other near-surface data, this structure is assumed for the entire southeast flank of Kilauea.

The $T_1 = 0.00 + \Delta/3.1$ and $T_1 = 0.00 + \Delta/3.7$ travel-time segments recorded at Naalehu from shots to the northeast and southwest respectively suggest that the 1.8-

TABLE 3

TRAVEL TIMES ALONG THE KAU-PUNA COAST

Refraction Unit	Bearing of Shots from Unit	Travel-time Curves	Distance Interval Recorded (km)
Naalehu	Northeast	$T_1 = 0.00 + \Delta/3.1$	0–10
		$T_2 = 0.70 + \Delta/4.8$	15–32
		$T_3 = 2.80 + \Delta/7.1$	
		$T_4 = 3.50 + \Delta/8.0$	38–88
	Southwest	$T_1 = 0.00 + \Delta/3.7$	0–15
Pahala	Northeast	$T_1 = 0.00 + \Delta/3.1$ (assumed)	
		$T_2 = 0.50 + \Delta/4.8$	12–40
		$T_3 = 2.95 + \Delta/7.1$	
		$T_4 = 3.55 + \Delta/8.0$	40–68
	Southwest	$T_0 = 0.00 + \Delta/3.1$ (assumed)	
		$T_1 = 0.50 + \Delta/4.8$	16–33
		$T_3 = 2.45 + \Delta/6.0$	
Hilina Pali	Northeast	$T_0 = 0.00 + \Delta/1.8$, $T_1 = 0.73 + \Delta/3.1$ (assumed)	
		$T_2 = 1.50 + \Delta/4.2$	6–14
		$T_3 = 3.10 + \Delta/7.4$	14–50
	Southwest	$T_0 = 0.00 + \Delta/1.8$, $T_1 = 0.73 + \Delta/3.1$ (assumed)	
		$T_2 = 1.10 + \Delta/5.0$	10.30
		$T_3 = 2.75 + \Delta/7.1$	30–60
Kamoamoa	Northeast	$T_0 = 0.00 + \Delta/1.8$ (assumed)	
		$T_1 = 0.70 + \Delta/3.1$	3–7
		$T_2 = 1.60 + \Delta/5.3$	7–28
	Southwest	$T_0 = 0.00 + \Delta/1.8$ (assumed)	
		$T_1 = 0.70 + \Delta/3.1$	3–7
		$T_2 = 1.25 + \Delta/5.3$	7–45
Cape Kumukahi	Southwest	$T_0 = 0.00 + \Delta/1.8$, $T_1 = 0.70 + \Delta/3.1$ (assumed)	
		$T_3 = 1.75 + \Delta/6.5$	10–53
		$T_4 = 3.50 + \Delta/8.2$	53–73
		$T_4' = 2.10 + \Delta/7.5$	73–84

km/sec layer is thin or absent on the flank of the Mauna Loa rift zone, and that the 3.1-km/sec layer extends to the surface northeast of Naalehu and grades into a 3.7-km/sec layer southwest of Naalehu (Figure 10). If the 4.8-km/sec travel-time segments northeast of Naalehu and Pahala are regarded as being approximately reversed by the 5.3-km/sec travel-time segment southwest of Kamoamao, then a 5.1-km/sec layer underlies Naalehu at a depth of 1.5 km and dips to the northeast at about 2°

to a depth of about 2.5 km under Kamoamoa. The symmetry of the 5.3-km/sec travel-time segments on either side of Kamoamoa suggests that the 5.1-km/sec layer dips up to the northeast toward Cape Kumukahi from Kamoamoa. The larger intercept time (1.60 sec) of the 5.3-km/sec branch northeast of Kamoamoa suggests that the depth to the 5.1-km/sec layer may increase from 2.5 km just southwest of Kamoamoa to 3.2 km just northeast of Kamoamoa. The above near-surface velocity distribution is summarized on Figure 10.

Clear secondary arrivals recorded at Naalehu and Pahala from shots beyond about 28 km to the northeast define travel-time segments $T_3 = 2.80 + \Delta/7.1$ and $T_3 = 2.95 + \Delta/7.1$ respectively. First arrivals recorded from shots beyond about 30 km southwest of Hilina Pali define the travel-time segment $T_3 = 2.75 + \Delta/7.1$. Although each of these travel-time segments undoubtedly involves arrivals refracted from the same horizon, their respective propagation paths are sufficiently different that they cannot safely be treated as being reversed. Taking the P-wave velocity of the refracting horizon to be 7.1 km/sec and working with the Naalehu and Pahala travel-time segments individually yields a depth of about 7.7 km to the top of the 7.1-km/sec layer under both Naalehu and Pahala. The greater intercept time (2.95 sec) for the Pahala 7.1-km/sec travel-time segment may be accounted for by the greater depth to the 5.1-km/sec layer northeast of Pahala compared to that northeast of Naalehu. As is indicated below, the depth to the 7.1-km/sec layer southwest of Hilina Pali is about 6.7 km.

First arrivals recorded at Cape Kumukahi from shots between 10 and 53 km to the southwest define the travel-time segment $T_3 = 1.75 + \Delta/6.5$. Because no arrivals were recorded for shot distances less than 10 km, it is assumed that the near-surface velocity structure down to the 5.1-km/sec layer under Cape Kumukahi is essentially the same as that under Kamoamoa. The recording unit at Cape Kumukahi was located immediately north of the axis of the Kilauea east rift zone (Figure 1), and propagation paths between the shots along the coast and the recording unit approach the rift zone at small angles and cross the rift zone a few kilometers southeast of the recording unit.

The P-wave velocities of the material-refracting arrivals defining the 6.5-km/sec branch southwest from Cape Kumukahi remain uncertain. The travel-time curves that come closest to reversing the 6.5-km/sec branch were recorded by the summit seismograph stations from shots along the southern edge of the east rift zone. These travel-time curves will be discussed in a subsequent paper, but it is worth noting that they suggest that the P-wave velocity of the core of the lower east rift zone (that part of the rift zone east of Makaopuhi) may be as low as 6.3 km/sec, significantly lower than the P-wave velocities of 7.0 km/sec determined for the shallow cores of the Kohala and Mauna Kea rift zones.

A simple three-layer solution of the 6.5-km/sec branch from Cape Kumukahi that assumes the P-wave velocity of the refracting horizon to be 6.3 km/sec indicates that the 6.3-km/sec layer is 4.5 km deep under Cape Kumukahi and dips to the northeast at about 2.5°. Alternatively, assuming a P-wave velocity of 7.0 km/sec for the refracting horizon, the 7.0-km/sec layer is about 3.2 km deep and dips about 4° to the southwest. Both solutions are shown on Figure 10. However, because the geometry of the 6.3- to 7.0-km/sec boundary is probably highly three dimensional, and because the axis of the east rift zone progressively diverges from the coast from Cape Kumukahi to the southwest, the simple two-dimensional solutions presented in Figure 10 suggest only an approximate range of possible solutions in the plane of the figure.

Strong secondary arrivals recorded from shots between 28 and 53 km southwest of Kumukahi are interpreted as reflections from the M discontinuity. These secondary

arrivals, together with first arrivals from a shot 73 km southwest of Cape Kumukahi, define the P_n travel-time segment $T_4 = 3.50 + \Delta/8.2$ mentioned earlier.

P_n arrivals recorded at Cape Kumukahi from shots between 73 and 84 km to the southwest are advanced by about 0.6 sec with respect to $T = 3.50 + \Delta/8.2$. Beyond 84 km southwest of Cape Kumukahi, the P_n arrivals have an apparent velocity of 7.5 km/sec. Similar variations are not evident on the "reversed" or "overlapping" travel-time curves recorded by the other units, and therefore the source of the variation remains uncertain.

There are three plausible explanations for the observed P_n perturbations: (1) a structural step or ramp on the M discontinuity 10 to 15 km northeast of Pahala, (2) near-surface velocity variations in the vicinity of Pahala, and (3) deep crustal velocity variations—probably associated with the Kilauea southwest rift zone.

On the basis of the existing data, the third possibility seems to offer the best explanation. Structure on the M discontinuity 10 to 15 km northeast of Pahala should show up as a travel-time perturbation on the P_n segment northeast from Naalehu. This travel-time segment is defined by good first arrivals, and a significant travel-time perturbation is not evident. Both deep crustal and near-surface velocity variation should show up on the "reversed" 4.8- and 5.3-km/sec travel-time segment from Naalehu and Kamoamoa. Again, perturbations are not evident on these travel-time segments, but the expected perturbations could conceivably be lost in the coarse data spacing or a misidentification of phases at the cross-over distances on the travel-time curves.

The recording unit at Hilina Pali was located about 11 km south of Kilauea caldera in the pie-shaped zone formed by the east and southwest rift zones and on the high side of the 500 m scarps of the Kilina Pali fault system (Figure 1). The travel-time curves recorded at Hilina Pali resemble the travel-time curves recorded by the summit seismograph stations (West Pit, Ahua, Mauna Loa, and Makaopuhi) rather than those recorded by the other four refraction units along the coast.

First arrivals recorded from shots between 6 and 10 km northeast and southwest of Hilina Pali define travel-time segments with apparent velocities 4.2 and 5.0 km/sec respectively. These arrivals have probably been refracted from a horizon about 2 km deep corresponding to the 5.1-km/sec horizon between Pahala and Kamoamoa. The low apparent velocity of the 4.2-km/sec segment may be due to a component of dip to the southwest on the 5.1-km/sec layer or to a badly fractured zone in the 5.1-km/sec layer associated with the Hilina Pali fault system. Of the two, a fracture zone seems the more plausible.

First arrivals recorded from shots beyond 14 km to the northeast and 30 km to the southwest define travel-time segments with apparent velocities 7.4 and 7.1 km/sec respectively. Assuming that the arrivals forming the 7.4- and 7.1-km/sec travel-time segments have been refracted from a 7.1-km/sec layer, the top of this layer is about 7.5 km deep 7 km northeast of Hilina Pali and about 6.7 km deep some 10 km southwest of Hilina Pali. The 7.1-km/sec horizon dips up to the northeast from Hilina Pali from 5° to 10°, depending on the attitude of the near-surface layers in the plane of wave propagation and has little or no dip to the southwest. The structure on the 7.1-km/sec layer inferred from the Hilina Pali travel-time curves is shown on Figure 10 (by dashed lines with parenthetic velocities) and is supposed to be somewhat behind, or inland from, the structure established by the four other recording units.

Kilauea and Mauna Loa structure from P_n delays. P_n arrivals from the three SAILOR HAT events detonated on Kahoolawe and recorded on the HVO seismograph network provide additional evidence on crustal structure under the summits of both Kilauea

and Mauna Loa. As shown on Figure 8 and Table 4, the P_n arrivals recorded on the summits of Kilauea and Mauna Loa are 0.4–0.6 and 0.2 sec early respectively with respect to the $T = 3.30 + \Delta/8.2$ P_n travel-time segment defined by stations along the Kona coast.

The propagation paths from the shotpoint on Kahoolawe approach the HVO seismograph stations from the northwest. The emerging sections of the P_n-ray paths cover horizontal distances of 10 to 25 km between the M discontinuity and the respective seismograph stations, and in most cases have sampled sections of the crust for which there is little or no independent information on structure. Thus the P_n delay data can-

TABLE 4

P_n DELAYS AT STATIONS ON HAWAII FROM THE SAILOR HAT EVENTS ON KAHOOLAWE

Station	$\Delta T = T - (3.30 + \Delta/8.20)$ sec			Avg. ΔT (sec)	Elevation (km)
	Shot number 1	Shot number 2	Shot number 3		
B2W		0.13		0.13	0.85
B2E		0.05		0.05	0.63
B3W		0.08		0.08	0.02
B3E		0.02		0.02	0.02
P3E		−0.07		−0.1	0.19
P3W		−0.02		−0.0	0.26
Ke			−0.08	−0.1	0.50
Hi			0.27	0.3	0.02
NB	−0.20		−0.11	−0.2	4.00
ML	−0.10	0.09	−0.10	−0.1	2.01
BIN	−0.34			−0.34	1.12
BIS	−0.53			−0.53	0.95
BIE	−0.58			−0.58	1.00
WP	−0.90			−0.9	1.12
NP	−0.55	−0.35	−0.55	−0.5	1.12
U	−0.40	−0.28	−0.38	−0.4	1.24
A	−0.57	−0.39	−0.59	−0.5	1.07
D	−0.50	−0.16	−0.56	−0.4	0.82
MP	—	—	—		0.88

not be used to give a unique velocity-depth distribution under the seismograph stations; they can, however, be used to suggest a range of possible crustal thicknesses for reasonable crustal velocities.

In this discussion average crustal velocity, V_a, is defined in terms of total crustal thickness, H, and P_n delay time, t, by

$$t = \frac{H(1 - V_a^2/V_n^2)^{1/2}}{V_a} = \sum_{i=0}^{n-1} \frac{h_i(1 - V_i^2/V_n^2)^{1/2}}{V_i}$$

where

$$H = \sum_{i=0}^{n-1} h_i ,$$

V_i is the P-wave velocity of crustal layers $i = 0$ through $n - 1$ each of thickness h_i, and V_n is the P-wave velocity of the upper mantle.

If the crust throughout the Kilauea summit area can be roughly approximated by a 5.1-km/sec "layer" over a 7.1-km/sec "layer" over an 8.1-km/sec upper mantle such that the average crustal velocity, V_a, is 6.5 km/sec (a value suggested by preliminary interpretation of Kilauea seismograph network arrivals from offshore explosions), then the P_n-delay data suggest: (a) the depth to the base of the crust decreases from about 13 km below sea level 18 km northwest of the summit of Kilauea to 11 km below sea level 7 km northwest of the summit, and (b) the depth to the top of the 7.1-km/sec "layer" decreases from about 4.5 km below sea level 5 km northwest of the summit to 3 km below sea level directly under the summit.

This interpretation agrees with Ryall and Bennett's (1968) analysis of the reversed profiles across the summit of Kilauea between Hilo and South Point in the sense that the depth to both the M discontinuity and the high-velocity crustal "layer" is less under the summit than under the flanks of Kilauea. However, it is likely that the assumption of constant average crustal velocity used in interpreting the P_n-delay data is not entirely appropriate. In particular, the stack of fossil magma chambers filled with ultrabasic crystal accumulates suggested by E. D. Jackson (1968) on the basis of his detailed study of xenoliths may well form a central cylindrical core of higher P-wave velocity than the dense system of dikes and sills in which it is presumably enclosed. A higher average crustal velocity under the summit of Kilauea would admit a larger crustal thickness for a given P_n delay time, but the horizontal distance covered by the emerging ray would also be larger.

Thus if we consider the -0.5 sec P_n delay recorded at Ahua, which gave the 11-km depth for the base of the crust 7 km northwest of the summit under the first interpretation, and assume that the appropriate average crustal velocity is 6.7 km/sec for this ray path, the depth to the base of the crust will be 13 km below sea level 15 km northwest of the summit. In other words, using this approximate method of interpretation and the given array of stations, we can say that if the average crustal velocity is roughly constant through out the summit area, the depth to the base of the crust is less under the summit area than under the flank, but if the average crustal velocity is higher under the summit region than in the surrounding flanks, we can say little about the depth to the base of the crust directly under the summit.

P_n arrivals from the SAILOR HAT events recorded on the North Bay seismograph on the summit of Mauna Loa (elevation, 4.0 km) average 0.2 sec early with respect to $T = 3.30 + \Delta/8.2$. The emerging section of the ray path between Kahoolawe and the summit of Mauna Loa leaves the M discontinuity in the vicinity of the saddle between Mauna Loa and Hualalai. If the average depth to the 7.0-km/sec horizon under the summit of Mauna Loa is about 7 km (3 km below sea level), as suggested by the North Bay travel-time curve from the Kona seismic-refraction shots (Figure 9), then the 0.2 sec P_n delay from the Kahoolawe shots requires that the M discontinuity be only about 10 km below sea level under the saddle, which seems a little thin. On the other hand, if the M discontinuity is 14 to 16 km below sea level under the saddle (total crustal thickness 18 to 20 km), the average crustal velocity must be between 6.7 and 6.9 km/sec and the 7.0-km/sec horizon must be only 2.0 to 3.6 km beneath the summit (0.4 to 2.0 km above sea level). Additional data will be required to resolve between these or other possibilities.

Discussion

The interpretation of the seismic-refraction data presented above can be summarized as follows:

(1) The depth below sea level to the M discontinuity is about 12 km under the northeast and southeast coasts of Kilauea and varies from about 18 km under the west coast of Mauna Loa to about 14 km under the west coast of Hualalai and Kohala Mountain. The depth to the M discontinuity under the northeast coasts of Mauna Kea and Kohala Mountain is probably about 15 km, but could be anywhere between 12 and 20 km, depending on the average P-wave velocity of the crust. The depth to the M-discontinuity appears to increase by 2 or 3 km toward the center of the island from the coasts, but the depth to material with mantle-like velocities (>7.5-km/sec?) may be as little as 10 km under the summit of Kilauea.

(2) The P-wave velocity (P_n) of the upper mantle under Hawaii is 8.2 ± 0.1 km/sec. The travel-time curves suggest that P_n is about 8.2 km/sec under most of the island and 8.1 km/sec under the southeast coast of Kilauea.

(3) The crust can be divided into two principal "layers" on the basis of P-wave velocities: (1) an "upper layer" with P-wave velocities increasing from 1.8 to 3.3 km/sec at the surface to 5.1 to 6.0 km/sec at depth, and (2) a "basal layer" with P-wave velocities between 6.3 to 7.2 km/sec. Geologically, the "upper layer" can be identified with the accumulated pile of lava flows that form the bulk of the island. The "basal layer" can be identified with two and possibly three geologically distinct structures all having similar P-wave velocities: (1) the original oceanic crust, (2) a dense intrusive system of dikes and sills associated with the central vents and rift zones of each volcano, and (3) a stack of floored magma chambers filled with ultramafic cumulates associated with the central vent of each volcano as postulated by Jackson (1968) on the basis of xenolith texture and distribution. Within the resolution of the data presented in this paper, it appears that the dense intrusive system (which may include an ultramafic cumulus core) extends from the top of the oceanic crust to within 3 km of the surface under the central vents and major rift zones of the volcanoes. The horizontal dimensions of the intrusive system appear to increase with depth, and at depth it is not possible to distinguish between the top of the oceanic crust and the broad base of the intrusive system. The resulting impression is that the "basal layer" increases in thickness toward the central vents and rift zones.

The following discussion involves some inferences relating the above interpretation of the seismic-refraction data to geologic structures and processes in Hawaii. At this stage, such inferences are necessarily speculative and should be read with this in mind.

On the basis of exposures in the deeply eroded Koolau rift zone on Oahu (Wentworth and Jones, 1940), it seems evident that at least the upper sections of the dense intrusive system consists of a dike swarm that has completely displaced the surrounding flows to form a solid mass of dike upon dike. Birch (1960) reports that P-wave velocities in diabase (whose physical properties should roughly correspond to those of the dike rocks) vary between 6.4 and 6.9 km/sec at pressures between 1 and 4 kb. The lava flows exposed on Kohala Mountain and Mauna Kea are rich in feldspar (Powers, 1955; Stearns and Macdonald, 1946, p. 160, 178), and it is possible that the slightly higher P-wave velocity (7.0 km/sec) suggested by the seismic-refraction data for the Kohala-Mauna Kea rift zones is due to residual olivine and pyroxene left behind by these feldspar-rich flows in scattered "pods" or in the floored chambers as postulated by Jackson (1968). Jackson (personal communication, 1968) suggests it is likely that the profile along the northern part of the Hamakua coast intersects the stack of floored chambers associated with the central vent of Kohala Mountain, which he believes may have an areal radius of 5 to 10 km.

The dense section of the dike swarm exposed on the Koolau rift zone is only 3 to 4 km wide, and all of the dikes are nearly vertical. It seems plausible that a similar situation should exist at shallow depths under the rift zones of the volcanoes on Hawaii. The tendency of the horizontal dimensions of the intrusive system to increase with depth implied by the seismic-refraction data may be due to: (1) the successive horizontal displacement of earlier dikes by the intrusion of later dikes as the volcano grows and/or (2) the migration of the active axis of a rift zone with time (the eastward offset of the sourthern end of the south rift zone of Mauna Loa may be a current example of such a process—see Figure 1).

McBirney (1963) and Nayudu (1962) have suggested that lava in early submarine eruptions of oceanic volcanoes may be largely insulated from direct contact with the ocean by a relatively buoyant water-saturated sedimentary layer or an initial mound of tuff and breccia. They conclude that under such circumstances, the early eruptions of the incipient volcano would result in broad laccolith-like bodies in which the physical properties of the cooled lava would be similar to those in a thick dike or sill. Such bodies may form the original cores upon which the superstructure of the Hawaiian volcanoes is built and would explain the apparent broad base of the intrusive system as it merges with the oceanic crust at depth.

On the basis of ground-tilt measurements made around the summit of Kilauea before and after the 1959–1960 eruption, Eaton (1962) calculates that a shallow magma chamber is centered at a depth of about 4 km beneath the summit of Kilauea. The seismic-refraction and P-wave delay data together with recent gravity measurements made by W. T. Kinoshita (personal communication, 1966) indicate that the 6.8- to 7.0-km/sec core extends to within less than 3 km of the surface under the summit of Kilauea, and thus that the shallow magma chamber is included within the dense, high-velocity core of the volcano. The large positive gravity anomalies and early P-wave arrivals associated with the summits of the other volcanoes, together with the ultramafic cumulus textured xenoliths found in summit cinder cones on volcanoes in the alkalic state (Jackson, 1968) suggest that similar magma chambers are included within all Hawaiian volcanoes, although the magma chambers of the older volcanoes are no doubt partially or completely crystallized.

The nature of the upward "bulge" of material with mantle-like velocities under the summit of Kilauea suggested by one interpretation of the P_n delay data is puzzling. The data presented in this paper provide little evidence for block faulting of the entire crust beneath the rift zones and summits of Mauna Loa and Kilauea postulated by Ryall and Bennett (1968) to explain both their interpretation of the seismic-refraction profiles between Hilo and South Point and Kinoshita's gravity data. As an alternative explanation for this apparent relief at the base of the crust under the summit of Kilauea (and possibly the other volcanoes), I suggest that at some time in the development of the volcano, the original oceanic crust in the vicinity of the central vents may have been completely disrupted and replaced by a system of large sills or magma chambers, and that this system of sills or magma chambers is now filled with ultramafic material accumulated through crystal settling. If the crystals settling in these early magma chambers were largely olivine, the P wave through these deep "fossil" chambers could well be within the range 7.5 to 8.0 km/sec.

One of the significant results brought to light by recent seismic-refraction studies is that the upper mantle P-wave velocity under most areas of Cenozoic volcanism is less than 8.0 km/sec, whereas that under normal oceanic crust or older, stable sections of the continental crust is greater than 8.0 km/sec (Pakiser and Steinhart, 1964). The

normal oceanic 8.2-km/sec P_n velocity under Hawaii together with the near-normal heat flow through the ocean floor around Hawaii reported by Sclater and Corry (1967) suggest that, at least for depths down to a few tens of kilometers, the geothermal gradient under Hawaii may not be significantly different than under normal regions of the Pacific Basin, and thus that the upper mantle under Hawaii may be dense, relatively cool, and competent compared to the upper mantle under other areas of active volcanism.

The isostatic condition of Hawaii can be estimated using the crustal structure obtained from the seismic-refraction measurements by comparing the mass per column of unit cross-sectional area between sea level and an assumed depth of compensation for the coastal sections of Hawaii with that for a "standard" oceanic crust. Assuming (1) that P-wave velocities are related to density according to the curves presented by either Nafe and Drake (*in* Talwani *et al*, 1959) or Woollard (1959), and (2) that the depth of compensation is 30 km below sea level, and taking the crustal structure near the proposed Mohole site (Shor and Pollard, 1964) as the standard oceanic section, I find that the crust-upper mantle section under the coasts of Hawaii has between 4×10^5 and 6×10^5 more mass per unit area (g/cm^2) than the standard oceanic crust (including, of course, the water layer). Thus if the "standard" oceanic crust is in approximate isostatic equilibrium—as seems reasonable from the near zero free-air gravity anomaly over the proposed Mohole site (Rose and Belshé, 1965)—the crust under the coasts of Hawaii is undercompensated. If the density contrast between the lower half of the crust under Hawaii and the upper mantle is 0.3 to 0.4 g/cm^3, then for compensation, the crust under the coastal sections would have to be 10 to 20 km thicker than indicated by the seismic-refraction results. Furthermore, for complete local compensation, the M discontinuity under the island would have to increase in depth by 6 to 8 km beyond its depth under the coasts for every kilometer of topographic elevation above sea level.

Clearly then, if the depth of compensation is about 30 km deep, the volcanic pile of Hawaii is to a large extent an uncompensated mass excess on the crust and upper mantle, and although the measured increase in crustal thickness under the island together with evidence for submergence of the coast lines (Apple and Macdonald, 1966) indicate that the crust under the island is subsiding in response to the excess load of the volcanic pile, the present subsidence is less than half of that required for isostatic equilibrium. This implied sluggish response to the excess load on the crust may well be related to a dense, high-velocity, and presumably cool and "viscous" mantle lid under Hawaii.

A cool upper mantle poses obvious problems with regard to a magma source for the active volcanoes of Hawaii. On the basis of swarms of earthquakes and "harmonic" tremor with foci 60 km beneath the summit of Kilauea proceeding the 1959 eruption, Eaton and Murata (1960) suggest that 60 km may be the depth at which magma enters the "plumbing system" of Kilauea. If it is, then the 8.2-km/sec section of the upper mantle may be a "layer" 40 to 50 km thick underlain by a hot, low-velocity layer in which partial melting of the mantle occurs.

Figure 11 is a generalized schematic section through the summit of a Hawaiian volcano based largely on data from Kilauea. This figure is intended only to illustrate the broad structural relations discussed above; it does not represent a particular profile along which actual measurements have been made. The left side of the figure shows the structure under a "normal" flank (generalized from the southeast flank of Kilauea), and the right side shows the structure under the axis of a major rift zone (the east rift zone of Kilauea). Recall that rift zones are linear features and thus that the structure a

few kilometers on either side of the rift zone, should approach that of a "normal" flank. The two principal seismic crustal layers—the upper "layer," which consists of the pile of lava flows, and the basal "layer," which includes the oceanic crust and the intrusive system—are shown by horizontal and vertical line patterns respectively.

Note that the most speculative part of the figure involves the structure under the summit, in particular the configuration of the present magma chamber and feeding conduit (solid outline), the stack of cumulus-filled fossil magma chambers suggested by Jackson (1968) (dashed outline), and especially the configuration and P-wave velocity of the high-velocity "bulge" and the position of the M discontinuity. The depth to the lower end of the feeding conduit at 60 km (the top of the low-velocity zone?) is based on Eaton and Murata's (1960) analysis of the 1959–60 eruption of Kilauea.

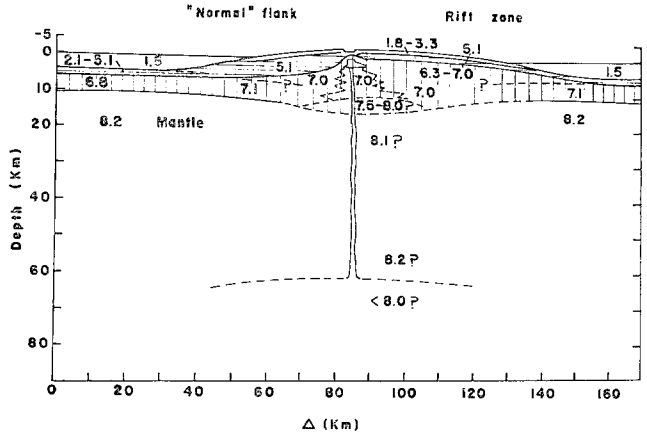

FIG. 11. Schematic cross-section showing idealized crustal structure of Hawaiian Volcano (based largely on Kilauea). Numbers indicate P-wave velocity in km/sec. The section to the right of the summit shows the structure under a major rift zone (the east rift zone of Kilauea), and the section to the left shows the structure under a "normal" flank (generalized from the southeast flank of Kilauea). The irregular shape under the summit represents the shallow magma chamber and main conduit of the volcano suggested by Eaton and Murata (1960) and a possible configuration of the cumulus-filled fossil magma chamber suggested by Jackson (1968). The suggested P-wave velocity decrease at 60 km is hypothetical.

ACKNOWLEDGMENTS

I would like to express my appreciation to the U. S. Coast Guard, without whose assistance this work would not have been possible. The enthusiasm shown by the Commanding Officer, Lt. T. H. Lloyd, and crew of the USCGC CAPE SMALL in carrying out the shooting operations was a major factor in the success of the program. I would like to thank the Commander of the Hawaiian Sea Frontier, U. S. Navy, for advising us on the scheduling of the SAILOR HAT events and supplying shot coordinates and times. I would also like to thank Dwight D. Pollard for permission to use times and locations of the Scripps Institution of Oceanography shots and Jerry Eaton for making available unpublished data he and Robert Koyanagi reduced from the HVO seismic network recordings of these shots.

REFERENCES

Adams, W. M. and A. S. Furumoto (1965). A seismic refraction study of the Koolau volcanic plug, *Pacific Science*, **19**, 296–305.

Apple, R. A. and G. A. Macdonald (1966). The rise of sea level in contemporary times at Honaunau, Kona, Hawaii, *Pacific Science*, **20**, 125–136.

Birch, Francis (1960). The velocity of compressional waves in rocks to 10 kolobars, Pt. 2, *J. Geophys. Res.* **65**, 1083–1102.

Eaton, J. P. (1962). Crustal structure and volcanism in Hawaii, The crust of the Pacific Basin, *Am. Geophys. Union Mon.* **6**, 13–29.

Eaton, J. P. and K. J. Murata (1960). How volcanoes grow, *Science*, **132**, 925–938.

Furumoto, A. S. and G. P. Woollard (1965). Seismic refraction studies of the crustal structure of the Hawaiian archipelago, *Pacific Science*, **19**, 315–319.

Furumoto, A. S., N. J. Thompson and G. P. Woollard (1965). The structure of Koolau volcano from seismic refraction studies, *Pacific Science*, **19**, 306–314.

Jackson, E. D. (1968). The character of the lower crust and upper mantle beneath the Hawaiian Islands: *23rd International Geolo. Cong.*, Prague, Czechoslovakia, 1968 (in press).

Kinoshita, W. T. (1965). A gravity survey of the Island of Hawaii, *Pacific Science*, **19**, 339–340.

Kinoshita, W. T., H. L. Krivoy, D. R. Mabey and R. R. MacDonald (1963). Gravity survey of the Island of Hawaii, in Geological SurveyResearch 1963, *U. S. Geol. Survey Prof. Paper* 475-C, C114–C116.

Macdonald, G. A. (1965). Hawaiian calderas, *Pacific Science*, **19**, 320–334.

Macdonald, G. A. and J. P. Eaton (1964). Hawaiian volcanoes during 1955, *U. S. Geol. Survey Bull.* 1171.

Manghnani, M. H. and G. P. Woollard (1965). Ultrasonic velocities and related elastic properties of Hawaiian basaltic rocks, *Pacific Science*, **19**, 291–295.

McBirney, A. R. (1963). Factors governing the nature of submarine volcanism, *Bull. Volcanologique* **26**, 455–469.

Menard, H. W. (1964). *Marine geology of the Pacific*, New York, McGraw-Hill.

Nayudu, R. Y. (1962). A new hypothesis for the origin of guyots and seamount terraces, Crust of the Pacific Basin, *Am. Geophys. Union Mon.* **6**, 171–180.

Okamura, A. T., R. Y. Koyanagi and H. A. Powers (1965). *Hawaiian Volcano Observatory Summary* 37.

Pakiser, L. C. and J. S. Steinhart (1964). Explosion seismology in the western Hemisphere, Chapter 5 in *Solid Earth and Interface Phenomena*. V. 2 of *Research in Geophysics*, edited by Hugh Odishaw, Cambridge, Mass., MIT Press, 123–147.

Pollard, D. D. and J. P. Eaton (1964). Crustal structure of the Island of Hawaii (abs.), *Geol. Soc. Am. Special Paper* **76**, 218.

Powers, H. A. (1955). Composition and origin of basaltic magma of the Hawaiian Islands, *Geochim. et Cosmochim. Acta* **7**, 77–107.

Raitt, R. W. (1956). Seismic-refraction studies of the Pacific Ocean basin, Pt. I, Crustal thickness of the Central Equatorial Pacific, *Bull. Geol. Soc. Am.* **67**, 1623–1639.

Richter, C. F. (1958). *Elementary Seismology*, San Francisco, W. H. Freeman and Co.

Rose, J. C. and J. C. Belshé (1965). Gravity and magnetic fields over the proposed Moho Hole site north of Maui, *Pacific Science*, **19**, 374–380.

Ryall, Alan, and Dale L. Bennett (1968). Crustal structure of southern Hawaii related to volcanic processes in the upper mantle, *J. Geophys. Res.* **73**.

Sclater, J. G. and C. E. Corry (1967). Heat flow, Hawaiian area, *J. Geophys. Res.* **72**, 3711–3715.

Shor, G. G. (1960). Crustal structure of the Hawaiian ridge near Gardner Pinnacles, *Bull. Seism. Soc. Am.* **50**, 563–574.

Shor, G. G. and D. W. Pollard (1964). Mohole site selection studies north of Maui, *J. Geophys. Res.* **69**, 1627–1637.

Stearns, H. T. and G. A. Macdonald (1946). Geology and ground-water resources of the Island of Hawaii, *Hawaii Terr. Div. Hydrography Bull.* **9**.

Talwani, M., G. H. Sutton and J. L. Worzel (1959). A crustal section across the Puerto Rico Trench, *J. Geophys. Res.* **64**, 1545–1555.

Warrick, R. E., D. B. Hoover, W. H. Jackson, L. C. Pakiser, Jr. and J. C. Roller (1961). The specification and testing of a seismic-refraction system for crustal studies, *Geophysics*, **26**, 820–824.

Wentworth, C. K. and A. E. Jones (1940). Intrusive rocks of the leeward slope of the Koolau Range, Oahu, *J. Geol.* **48** (8, pt. 2), 975–1006.

Woollard, G. P. (1951). A gravity reconnaissance of the island of Oahu, *Trans. Am. Geophys. Union*, **32**, 358–368.

Woollard, G. P. (1959). Crustal structure from gravity and seismic measurements, *J. Geophys. Res.* **64**, 1521–1554.

National Center for Earthquake Research
U. S. Geological Survey
Menlo Park, California

Manuscript received March 18, 1968.